LPS-induced inflammatory responses and analysis of cardioprotective gene expression in mouse primary cardiac fibroblasts and cardiac myocytes

Mrinal Kumar Das

Norwegian University of Life Sciences
Department of chemistry, biotechnology and food science
Master Thesis 60 credits 2012

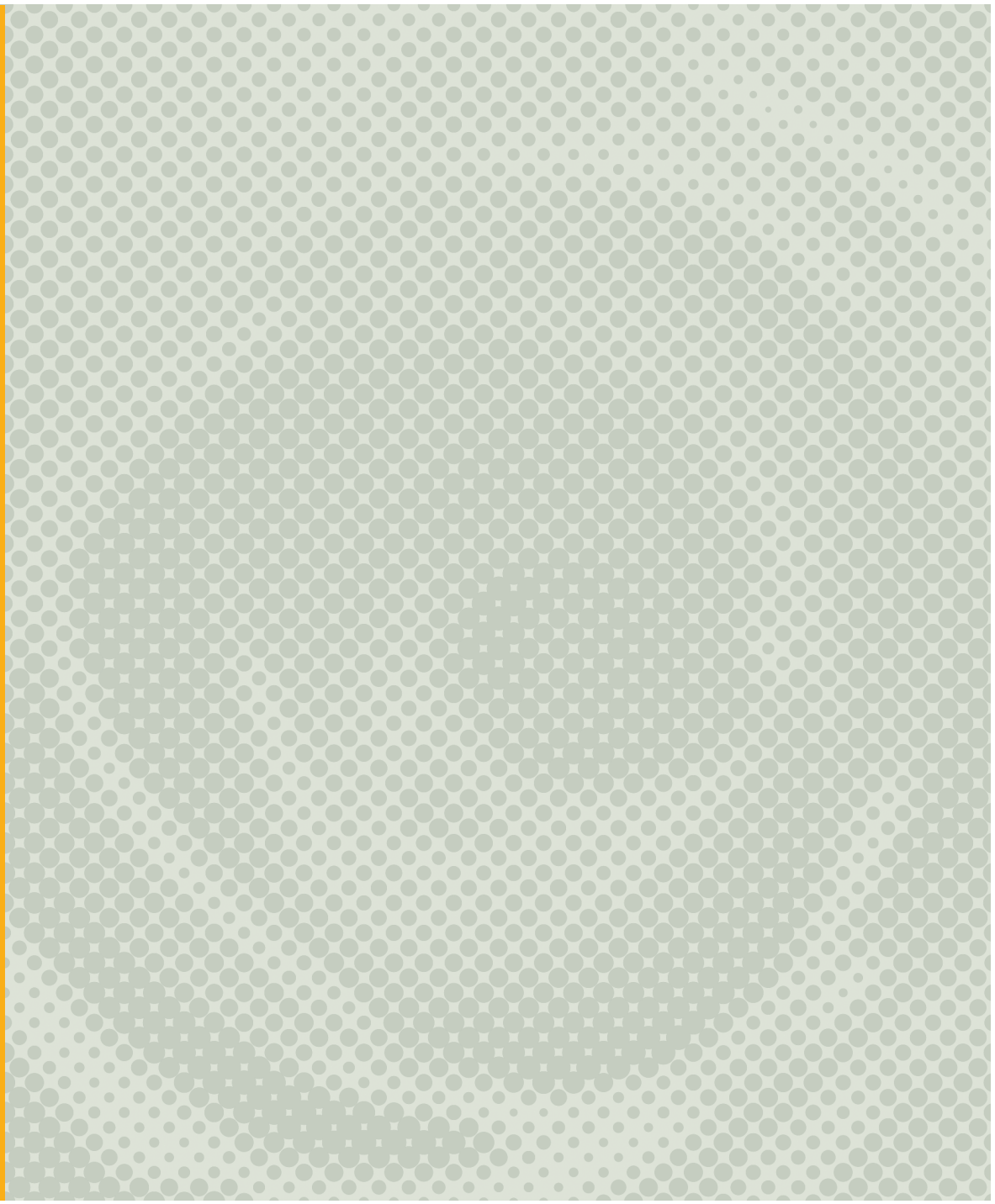

“LPS-induced inflammatory responses and analysis of cardioprotective gene expression in mouse primary cardiac fibroblasts and cardiac myocytes”

Performed at

Institute for Surgical Research,

Oslo University Hospital Rikshopitalet.

December 2012

By

Mrinal Kumar Das

ACKNOWLEDGEMENTS

The present work was carried out at Institute for Surgical Research, Department of Cardiology, Oslo University Hospital Rikshospitalet under the supervision of Senior Scientist Md. Shakil Ahmed, PhD and Professor Håvard Attramadal, MD.

I would like to thank all the members of the Molecular Cardiology Group for the time and knowledge they all have provided. Particularly, I am very grateful to Dr. Shakil Ahmed and Professor Håvard Attramadal for their professional guidance throughout the whole work and always having the time to help me despite their busy schedule. I would also pay my gratitude to my internal supervisor Tor Lea for his invaluable guidance and assistance.

Finally, I would extend my gratitude to my beloved parents and my siblings for their regular inspiration and support.

Ås, December, 2012

Mrinal Kumar Das

ABSTRACT

Sepsis, an uncontrolled inflammatory response is an important cause of death among the critically ill patients. Several lines of evidences have confirmed depression of myocardial function in sepsis which led researchers to focus intensely on myocardial dysfunction in sepsis. Several studies reported that LPS-induced pro-inflammatory cytokines, TNF-α and IL-1β play a key role in sepsis-induced myocardial dysfunction. On the contrary, the secreted CCN matricellular proteins, in particular CCN2/CTGF (connective tissue growth factor), CCN5/WISP-2 (Wnt1-inducible signalling pathway protein-2) and the TGF-β superfamily cytokine, GDF-15 were shown to play cardioprotective roles in cardiac dysfunction and remodelling. In our present study, the effects of LPS have been investigated in adult mouse cardiac fibroblasts and cardiac myocytes. We assessed the mRNA levels and the protein levels of TNF-α, IL-1β, CCN2, CCN5 and GDF15 in the absence or presence of LPS in the adult mouse primary cardiac fibroblasts and cardiac myocytes by real-time q-PCR and Western blot analyses. We also investigated the viability of adult mouse primary cardiac myocytes after exposure to LPS (0.1 μg/ml and 10 μg/ml) for different periods of time (0, 3,6,12 and 24 hours) by trypan blue exclusion assay. Real-time q-PCR demonstrates induction of mRNA levels of TNF-α and IL-1β in LPS-treated adult mouse cardiac fibroblasts and myocytes. Particularly, in cardiac fibroblasts the induction of mRNA expressions of TNF-α and IL-1β were found to be much more robust than that in cardiac myocytes. Western blot analysis of extracts of cardiac fibroblasts revealed that the precursor protein levels of both TNF-α and IL-1β were significantly induced in the LPS stimulated cardiac fibroblasts compared to non-stimulated cells. However, in cardiac myocytes the precursor protein levels of TNF-α and IL-1β remained unchanged in LPS-treated cells compared to control cells. In addition, gene expression analysis revealed down-regulation of CCN2 and CCN5 in LPS stimulated cardiac fibroblasts, whereas mRNA levels of GDF15 were found to be up-regulated in LPS-treated cardiac myocytes. Assessment of LPS-induced cell death of adult cardiac myocytes demonstrates significant decrease of cell viability in LPS-treated cardiac myocyte cultures. In our future studies, we will investigate the cytoprotective effects of recombinant CCN2, CCN5 and GDF15 at LPS-induced cell death in cardiac cell cultures. It would also be interesting to delineate the effects of LPS *in vivo* using CCN2-transgenic mouse model with cardiac specific overexpression of CCN2.

ABBREVIATIONS

SIRS	Systemic inflammatory response syndrome
LVSWI	Left ventricular stroke work index
TTE	Transthoracic echocardiography
LVEF	Left ventricular ejection fraction
TEE	Transesophageal echocardiography
LPS	Lipopolysaccharide
TNF-α	Tumor Necrosis Factor-α
IL-1β	Interleukin 1β
CTGF	Connective Tissue Growth Factor
WISP2	Wnt-1 Inducible Signalling Pathway 2
GDF15	Growth Differentiation Factor 15
NO	Nitric Oxide
TLR-4	Toll Like Receptor-4
LBP	LPS Binding Protein
MD-2	Myeloid Differential Protein-2
CD-14	Cluster of Differentiation-14
LV	Left ventricle
SERCA2a	Sarcoplasmic reticulum Ca^{2+} ATPase
iNOS	inducible Nitric Oxide Synthase
ECM	Extracellular Matrix
PDGF	Platelet-derive Growth Factor
AT-1	Angiotensin-II type 1
IGFBD	Insulin-like Growth Factor Binding Domain
vWC	von Willebrand factor type-C
TPS-1	Thrombospondin Type-1
CT	C-terminal
TGF-β	Transforming Growth Factor
FAM	6-carboxy fluorescin dye
NFQ	Nonfluorescent quencher
FRET	Fluorescence Resonance Energy Transfer
RT	Reverse Transcription
GAPDH	Glyceraldehyde 3-phosphate Dehydrogenase

SDS	Sodium Dodecyl Sulfate
PVDF	Polyvinylidene Fluoride
HRP	Horseradish Peroxidase
qPCR	Quantitative Polymerase Chain Reaction
ROS	Reactive Oxygen Species

Table of Contents

1. INTRODUCTION

1.1 Sepsis

According to prevailing theory, sepsis is an uncontrolled inflammatory response [1-3]. In 1879-80, Luis Pasteur discovered for the first time that bacteria existed in blood from patients with puerperal septicemia. Survival of a woman led Pastuer to articulate "Natura medicatrix won the victory", a notion that body responds systematically to sepsis to fight off the pathogens (Fig. 1.1). However, sepsis has now appeared as an important cause of death in critically ill patients [4]. The occurrence of sepsis is increasing every year and lately it has been published as 132 per 100000 populations with 50% mortality approach [5].

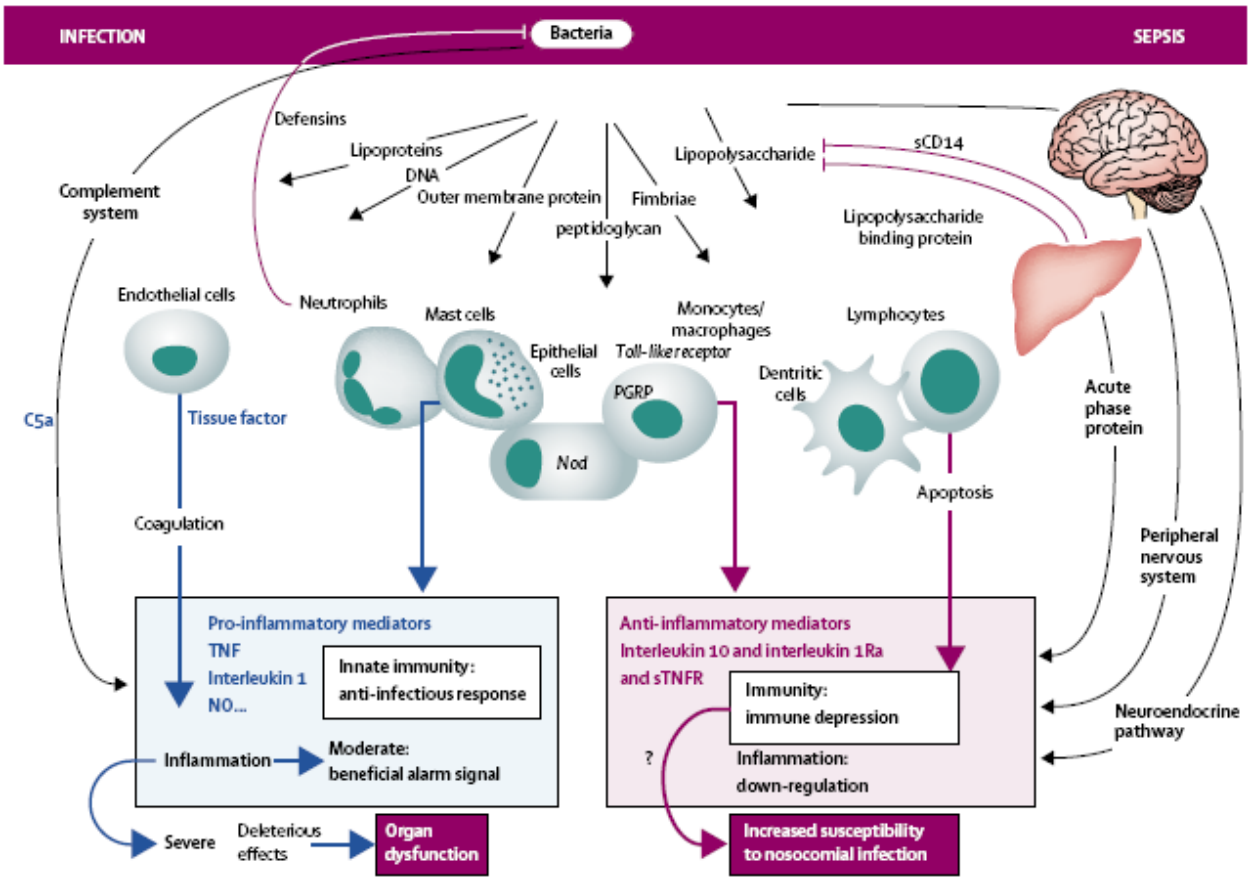

Figure 1.1 From bacteria to disease [6]. Barred lines = Inhibition and Arrows = Activation and consequences.

A consensus conference defined sepsis as "the systemic inflammatory response syndrome (SIRS) that occurs during infection [1]. " Table 1.1 quotes the current criteria to establish the

diagnosis of systematic inflammatory response syndrome (SIRS), sepsis and septic shock [1, 6].

Table 1.1

SIRS A response from the body to an infectious or noninfectious insult. It has actually pro and anti-inflammatory components though the definition refers to it as an ‘‘inflammatory’’ response [7]. Two or more of the following conditions: ✓ Temperature >38.5°C or <35°C ✓ Heart rate >90 beats per minute ✓ Respiratory rate >20 breaths per minutes or Atrial CO_2 <32 mm Hg or need for mechanical ventilation ✓ White blood cell count >12 000/mm^3 or 4000/mm^3 or 10% < immature (band) forms
Sepsis SIRS and documented infection (culture or gram-stain of blood, sputum, urine, or normally sterile body fluid positive for pathogenic organisms; or focus for infection identified by visual inspection, e.g. ruptured bowel with free air or bowel contents found in the abdomen at surgery or a wound with purulent discharge)
Severe sepsis Sepsis and at least one of the signs of organ hypoperfusion or organ dysfunction: ✓ Areas of mottled skin ✓ Capillary refilling time ≥3 s ✓ Urinary output of <0.5 ml/kg for at least 1 h or renal replacement therapy ✓ Lactate >2 mmol/L ✓ Abrupt change in mental status or abnormal electroencephalogram findings ✓ Platelet count <100000/ml or disseminated intravascular coagulation ✓ Acute lung injury/acute respiratory distress syndrome ✓ Cardiac dysfunction (echocardiography)

Septic shock Severe sepsis and one of the following conditions: ✓ Mean arterial pressure <60 mm Hg (<80 mm Hg if previous hypertension) after 20-30

ml/kg starch or 40-60 ml/kg saline solution, or pulmonary capillary wedge pressure between 12 and 20 mm Hg ✓ Need for dopamine >5 µg/kg.min or norepinephrine or epinephrine of <0.25 µg/kg.min to maintain mean arterial pressure above 60 mm Hg (80 mm Hg if previous hypertension)
Refractory septic shock Need for dopamine at >15 µg/ kg.min, or norepinephrine or epinephrine at >0.25 µg/kg.min to maintain mean arterial pressure .60 mm Hg (80 mm Hg if previously hypertensive)

1.2 Sepsis-induced Cardiac Dysfunction

In 1951, Waisbren first described that sepsis causes the cardiovascular dysfunction [8]. Recent evidences have confirmed depression of myocardial function in sepsis and reduced cardiac index or echocardiographic evidence of cardiac dysfunction are now considered essential criteria for diagnosis of severe sepsis [6, 9] which led researchers to focus intensely on myocardial dysfunction in sepsis.

The concept of depressed myocardial function in sepsis emerged from studies utilizing radionuclide cineangiography performed by Parker et al. in a group of septic shock patients. They showed significant depression of myocardial function [10]. Their group also showed that patients with severe sepsis and septic shock had intrinsically impaired myocardial performance as determined by assessment of left ventricular stroke work index (LVSWI) in response to fluid infusion [11]. Similar deviations appeared in the right ventricle [12]. Septic shock patient displays reduced left ventricular contractility (abnormal left ventricular stroke work index) and left ventricular dilatation.

More recently, echocardiography is used to characterize cardiac dysfunction in severe sepsis and septic shock. Several research data have stated impaired left ventricular systolic and diastolic function. In a longitudinal study, transthoracic echocardiography (TTE) showed significantly depressed left ventricular ejection fraction (LVEF) in all septic shock patients [13]. Transesophageal echocardiography (TEE) reported a 60% incidence of global left ventricular hypokinesia in a series of patients [14]. Acute and reversible left ventricular

dilatation with systolic left ventricular dysfunction was reported in a group of septic patients followed with serial TEE [15].

Cardiac depression during sepsis is probably multi-factorial. Early investigators claimed that myocardial ischemia was responsible for myocardial dysfunction though it has been excluded as a cause by subsequent studies. These studies reported that high coronary blood flow, net myocardial lactate extraction and diminished coronary artery–coronary sinus oxygen difference emerge during sepsis [16]. The microcirculation deviates during sepsis with endothelial disruption and misdistribution of blood flow [17]. Sepsis causing regional ischemia may also alter microvascular blood flow in the heart [18, 19].

A circulating myocardial depressant factor in sepsis was first proposed in the 1970s [20, 21]. In 1985, Parrillo et al. showed that serum obtained from patients with septic shock developed a significant depression in an "*in vitro* cardiomyocyte performance'' [22]. In a study of neonatal rat cardiac myocyte cultures, the ultrafiltrate from septic patients caused significantly higher amounts of pro-inflammatory cytokines and anaphylatoxins release, proposing an involvement of a number of circulating factors in sepsis-induced myocardial depression [23].

Endotoxin i.e., lipopolysaccharide (LPS) released by gram-negative bacteria is the key mediator of the cardiovascular dysfunction in septic shock [24]. After endotoxin administration in the heart, the typical haemodynamic pattern of severe sepsis developed with an increased heart rate, an increased cardiac index and a low systematic vascular resistance. After volume loading, a reduction in LVEF and LV performance developed [24]. Toll-like receptor-4 plays a pivotal role in endotoxin-induced cardiac dysfunction through activation of NF-KB pathway and causes the release of various cytokines and the progression of the inflammatory response [25, 26]. Several studies reported that the inflammatory cytokines, TNF-α and IL-1β play a key role in sepsis-induced myocardial dysfunction. The mechanism of TNF-α induced cardiac dysfunction is not well elucidated, but probably alteration of calcium homeostasis and increased synthesis of nitric oxide (NO) appear to be key players. IL-1β causes significant concentration-dependent depression of maximum extent and peak velocity of myocyte shortening [27]. NO has a direct effect on cardiac contractility [28-30]. Overproduction of NO adversely affects myocardial contractile function [31]. NO has also

been reported to depress myocardial energy production and cause apoptosis of cardiac myocytes [32, 33]. Sepsis induced cardiac dysfunction are given in a flow chart (Fig. 1.2)

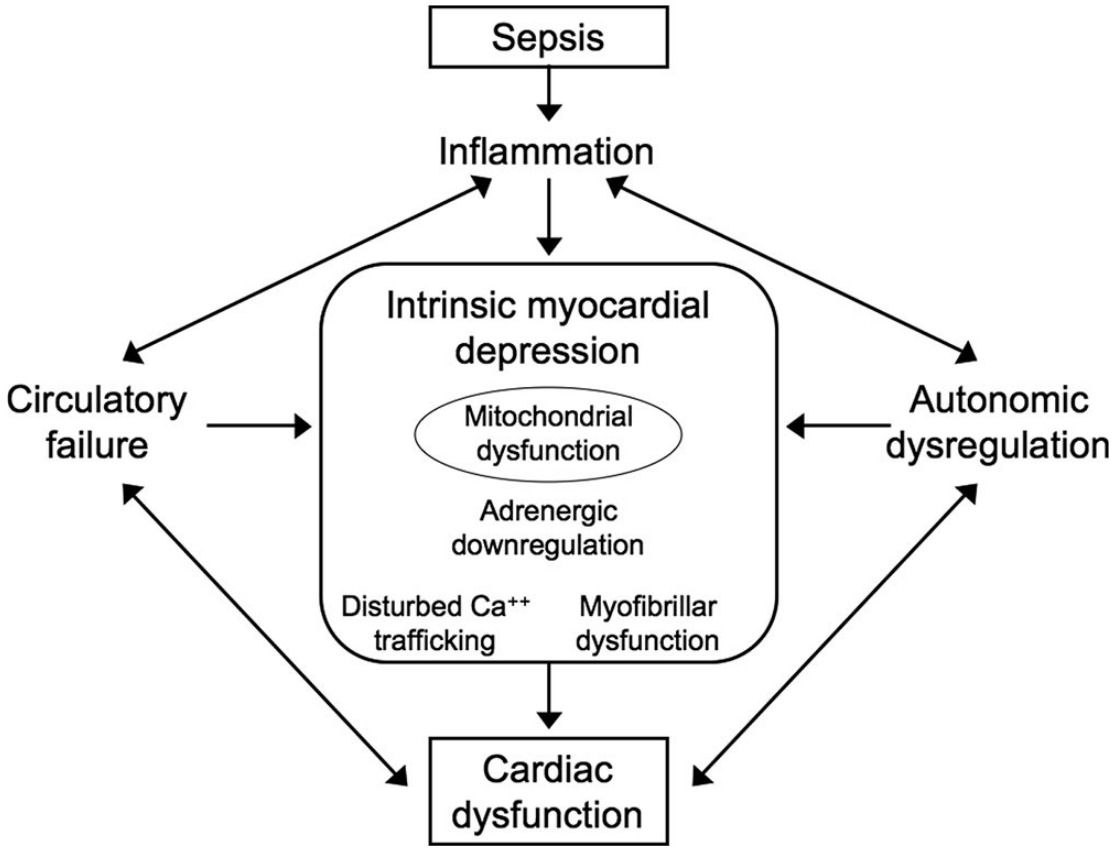

Figure 1.2 Sepsis-induced cardiac dysfunction. During sepsis changes in the macro and microcirculation, autonomic dysfunction, and inflammation-induced intrinsic myocardial depression impair cardiac performance. The mechanisms of myocardial depression include down-regulation of adrenergic pathways, disturbed intracellular calcium (Ca^{2+}) trafficking and impaired electromechanical coupling at the myofibrillar level. Mitochondrial dysfunction is thought to play a central role in this sepsis-induced organ dysfunction [34].

1.3 Endotoxin or Lipopolysaccharide (LPS)

Louis Pasteur (1822–1895) proved first beyond any doubt that microbes (the term 'microbiology' was created by Pasteur) can cause an infectious disease [35]. In 1886, Ludwig Brieger (1849–1919) discovered that germs secrete poisonous products, termed 'toxins', [36]. Robert Koch, who had identified *V. cholerae* in 1884, claimed that a poisonous substance played a pivotal role in cholera pathogenesis [37]. Koch encouraged one of his coworkers, Richard Pfeiffer (1858–1945), to investigate the nature of the toxins involved in cholera pathogenesis. During his studies, Richard Pfeiffer (1858–1910) discovered that

lysates of heat-killed bacteria of the cholera-inducing infectious agent *Vibrio cholerae* developed toxic shock reactions in guinea pigs and eventually the animals died [38]. Pfeiffer formulated the concept that *V. cholerae* consists of a heat-stable toxic substance in association with the insoluble part of the bacterial cell [39, 40] and he named this substance endotoxin (from the Greek 'endo' meaning 'within'). Pfeiffer proposed that both Gram-negative and Gram-positive bacteria consist of endotoxin. The Italian pathologist Eugenio Centanni (1863–1948), summarized Pfeiffer's work "Thus, we can conclude that the whole family of bacteria possesses essentially the same toxin … upon which depends the typical picture of the general disturbances caused by bacterial infections" [41]. Also, Centanni recognized the intimate relationship between the pyrogenic and toxic properties of endotoxin, which he found chemically inseparable. William B. Coley (1862–1936) showed that mixtures of killed bacteria (*Serratia marcescens* and *Streptococci spp.*) caused fever as well as induced remissions of certain malignant tumors in humans [42] which helped to discover tumor-necrosis factor (TNF) many years later.

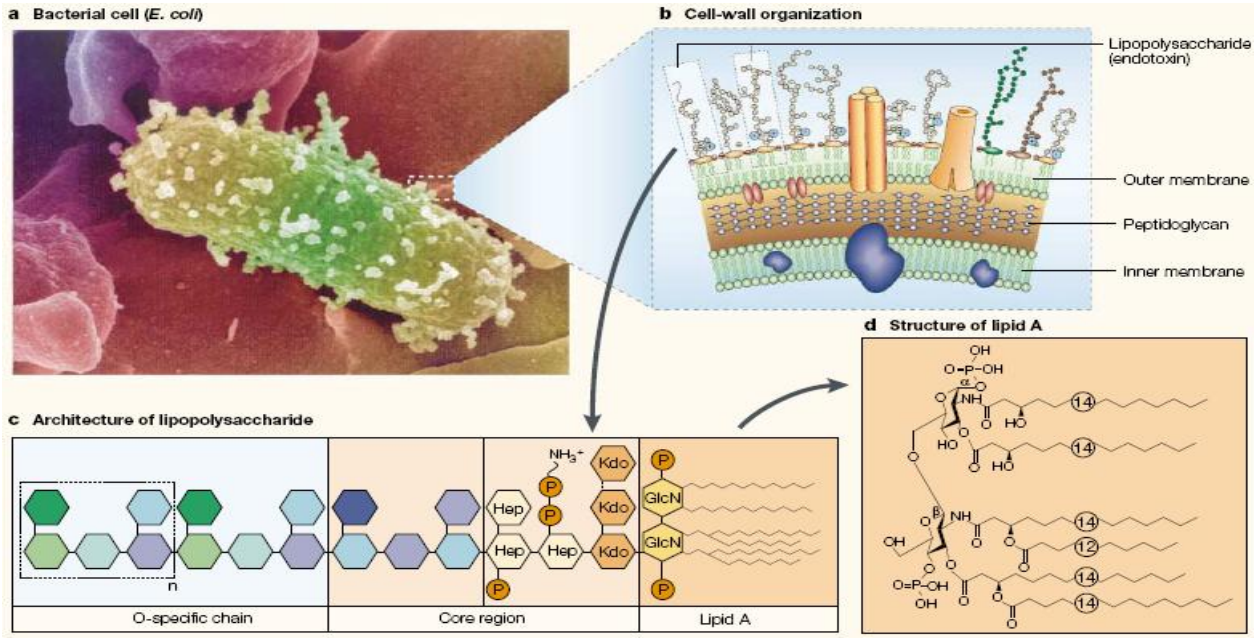

Figure 1.3 Gram-negative bacterium, *Escherichia coli* (a) with lipopolysaccharide (LPS; endotoxin) in the bacterial cell wall (b) and architecture of LPS (c) along with its toxic centre, the lipid A component (d) [43].

After intensive studies today we know that endotoxin is structurally an essential component of the outer membrane of gram-negative bacteria [44]. Lüderitz and Westphal designated this endotoxin as lipopolysaccharide (LPS) beacuse of its chemical composition [45]. It consists

of an amphipathic lipid A component and hydrophilic polysaccharides of the core and O-antigen [46, 47]. Several studies reported that lipid A had the toxic and pyrogenic properties of endotoxin [44]. Lipid A is a glycophospholipid, with unique structural features. For example, lipid A of Escherichia coli's LPS consists of a 1,4′-bisphosphorylated β1,6-linked D-glucosamine (D-GlcN) or a Glc2,3N disaccharide, which carries four residues of (R)-3-hydroxytetradecanoic acid at positions 2, 3, 2′ and 3′, two of which are acylated at the 3-hydroxy group by dodecanoic acid (2′) and tetradecanoic acid (2′). The hydroxy group at carbon 4 is free whereas that at 6′ is the attachment site for the polysaccharide component. Lipids A molecules of other gram-negative bacteria have the similar architectural principle though they may differ in structural details (Fig. 1.3) [48]. *E. coli* lipid A has more endotoxic effects than any other synthetic molecules although any modification of the structure of *E. coli* lipid A yielded products of lower endotoxicity. Therefore, bisphosphoryl lipid A is 100-fold more toxic than monophosphoryl lipid A (MPL), and A partial lipid A structure (lacking the two secondary acyl groups) is entirely devoid of toxicity in the human system [49].

Upon infection, LPS released from Gram-negative bacteria is first recognized by the host immune cells such as macrophages, neutrophils, mucosal epithelial cells and endothelial cells. This recognition initiates several intracellular signal transduction pathways i.e., cell activation and production of a variety of endogenous mediators, including pro-inflammatory cytokines, adhesion molecules, acute phase proteins, nitric oxide and prostaglandins [50, 51]. Abnormal host responses may contribute to tissue damage, organ failure i.e., symptoms characteristic of septic shock.

The Toll protein first discovered in Drosophila, plays a pivotal role in the determination of the dorsal–ventral patterning during embryogenesis [52, 53] which is an early form of defence in the innate immune system [54, 55]. The mammalian tolls like receptors (TLRs) are the first line of defence expressed by cells of the innate immune system. Lipid A is the main pathogen associated molecular pattern of LPS. Using the C3H/HeJ mouse strain Beutler's group demonstrated that TLR4 is a key sensor for LPS [52]. LPS stimulation of mammalian cells involves several proteins including the LPS binding protein (LBP), CD14, MD-2 and TLR4 [53, 56]. LBP is a soluble shuttle protein. LBP directly binds to LPS and mediates the association between LPS and CD14 [54, 55]. CD14 is a glycosyl phosphatidylinositol-anchored protein, which also exists in a soluble form. CD14 mediates the transfer of LPS to the TLR4/MD-2 receptor complex and regulates LPS recognition [50]. MD-2 is a soluble

protein and it non-covalently associates with TLR4. However, it can directly form a complex with LPS in the absence of TLR4 [57-59]. Although no evidence suggests that TLR4 can bind LPS directly, TLR4 can enhance the binding of LPS to MD-2 [60]. Therefore, LPS stimulation of TLR4, includes the participation of several molecules and the currently favored model is given below (Fig. 1.4) [56, 61]. MyD88 was first described as a myeloid differentiation primary response gene [62].

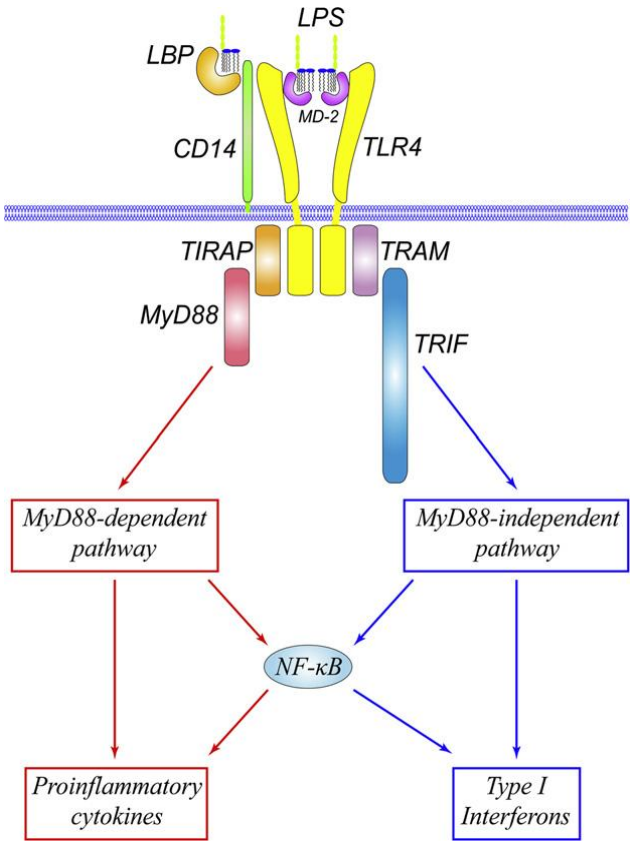

Figure 1.4 Overview of LPS/TLR4 signalling. LPS recognition is mediated by LBP and CD14 following by TLR4/MD-2 receptor complex. LPS/TLR4 signalling can be divided into MyD88-dependent and MyD88-independent pathways, which mediate the activation of pro-inflammatory cytokines and Type I interferon genes [51].

LPS plays a pivotal role in sepsis associated depression of myocardial function [63]. Suffredini et al. confirmed the development of cardiac dysfunction by giving endotoxin to healthy human volunteers [24]. Jianhui et al. interestingly demonstrated that altered volume loading conditions caused the septic cardiac abnormalities within 6 hours of LPS administration and LV (Left Ventricle) contractility increased at 6 hour period [64]. These data differ with previous murine studies that reported decreased myocardial contractility after LPS administration. However, mostly load-dependent indices of contractility were used to assess function, such as ejection fraction and maximal systolic pressure increment (dP/dtmax)

[65, 66]. This finding is consistent with previous studies. These studies also demonstrated reductions in loading conditions in dog and calves given LPS [67, 68].

LPS mediating tumor necrosis factor (TNF)-α and interleukin (IL)-1β, cause septic myocardial dysfunction through sarcoplasmic reticulum calcium leakage [69, 70]. Sarcoplasmic reticulum Ca^{2+} ATPase (SERCA2a) plays a pivotal role in cardiac function via maintenance of calcium homeostasis. TNF-α decreased SERCA2a expression via enhancing SERCA2a promoter methylation in HL-1 murine atrial cells [71]. Lancel et al. reported that LPS-induced proximal mediators of apoptotic response i.e. caspase activation, sarcomere destruction and contractile dysfunction in rat LV cardiomyocytes [72]. LPS also impaired SERCA and mitochondria-dependent calcium uptakes [73]. TLR-4 expressed in cardiomyocytes plays a key role in LPS-induced myocardial dysfunction [74]

1.4 Tumor Necrosis Factor (TNF)-α

TNF-α plays a key role in the pathogenesis and progression of myocardial ischemia/ reperfusion injury and heart failure [75]. It was first identified as an endotoxin-induced serum factor that caused necrosis of tumors [76]. TNF-α is a part of the innate immune system response to different forms of stress i.e., infection, trauma, ischemia/reperfusion (I/R). Normally TNF-α concentration is low both in the circulation and the heart in healthy individuals [77-79]. A enormous amount of preformed homotrimaric soluble TNF-α is released from macrophages, lymphoid cells, mast cells, endothelial cells (EC), fibroblasts within minutes by inflammatory stimuli i.e., bacterial (lipopolysaccharides and other products), viral [80], parasite infections [81-83] or acute injury, such as ischemia [84]. Acute myocardial I/R also causes a massive release of TNF-α from the heart [85-88]. Excessive TNF-α expression in the heart induces cell death, contractile dysfunction, dilated cardiomyopathy and fibrosis via TNF-α receptor type 1 [75].

1.5 Interleukin (IL)-1β

Interleukin (IL)-1β (15KD) is the prototypic, pro-inflammatory cytokine; able to induce a large portfolio of genes in a wide variety of cell types, usually not expressed in normal physiological condition [89]. It was first identified as the first “endogenous pyrogen” due to exerting fever-inducing effects in both rabbits and humans [90, 91]. Consistent induction and activation of IL-1β is observed in many inflammatory conditions and may contribute to

tissue injury in many diseases e.g., sepsis, rheumatoid arthritis and inflammatory bowel disease [92]. IL-1β increases the expression of inducible nitric oxide synthase (iNOS) and cyclo-oxygenase (COX)-2. IL-1β also increases many other cytokines expressions, such as TNF-α, the chemokines and adhesion molecules. In addition, IL-1β increases the expression of various tissue proteases and matrix metalloproteases and inhibits the synthesis of proteoglycans [93, 94]. IL-1β might be involved in atherothrombotic disease by mediating atheromatous lesions formation, vascular inflammation and plaque destabilization. IL-1β acutely regulates the inflammatory response in myocardial infarction and enhances the expression of matrix metalloproteinases following the development of adverse remodeling. IL-1β signaling might also be involved in cardiac dysfunction promoting myocardial hypertrophy and inducing cardiomyocyte apoptosis [95].

1.6 Connective Tissue Growth Factor (CTGF) or CCN2

CTGF belongs to a growing family of genes, called CCN family of genes. CCN proteins are modular and secreted extracellular matrix (ECM) associated proteins. They are involved in regulating miscellaneous cellular activities such as adhesion, migration, mitogenesis, differentiation, and survival. The acronym CCN was coined by Peter Bork in 1993 which stands for CYR61, CTGF, NOV, the first three proteins of CCN family of genes [96]. CCN proteins share 38 conserved cysteine residues with approximately 40 to 60% sequence similarity and about 30 to 50% overall amino acid sequence identity [97]. Connective tissue growth factor (CTGF) holds the second position among six CCN proteins. It has differently been known such as FISP12, Hcs24, ecogenin, IGM2, IGFBP8, IGFBP-rP2 and CCN2 [96, 98, 99]. Bradham et al. first isolated CCN2 from human umbilical vein endothelial cell culture supernatants using an anti-platelet-derive growth factor (PDGF) antibody. CCN2 is a 38 KD monomeric protein composed of 349 residues and its four distinct structural modules (Fig. 1.5) offer multi-functionality [100]. This glycoprotein is involved in diverse cellular responses including extracellular matrix production, cell proliferation and growth, cell adhesion, apoptosis, or cell viability depending on cell type and cellular context [101].

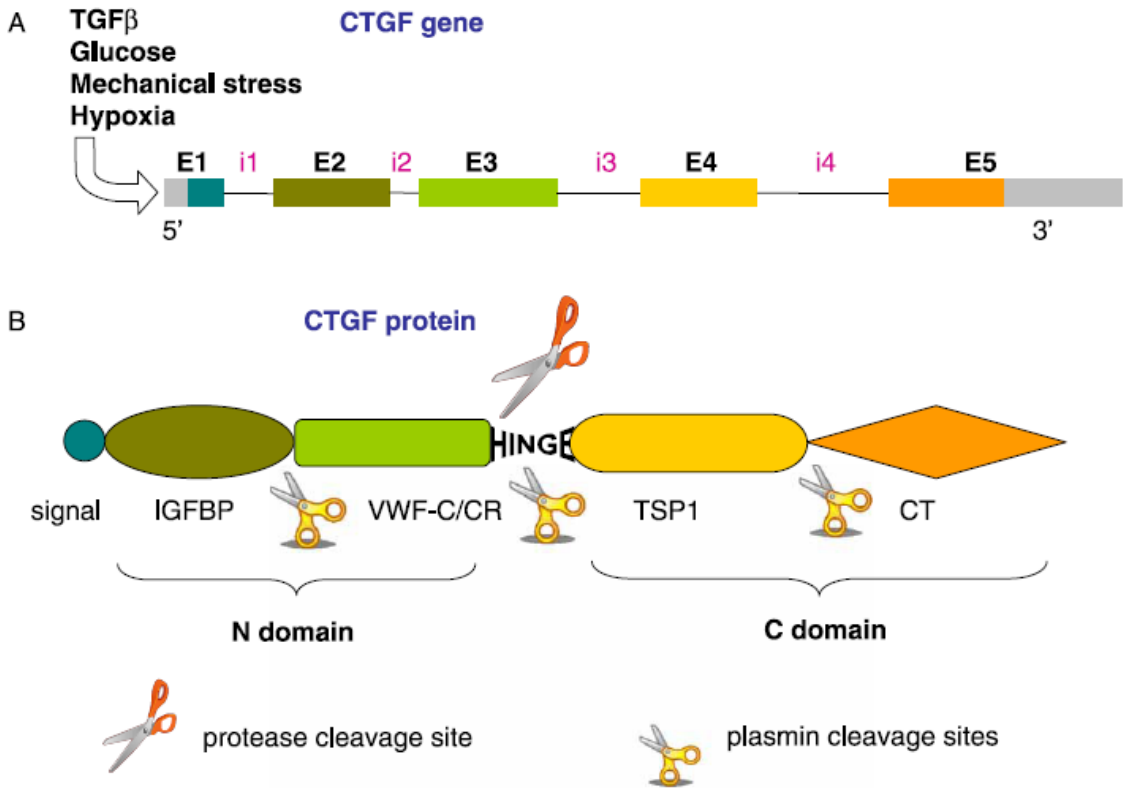

Figure 1.5 (A) CCN2 gene structure downstream of the transcription start site. Grey bars indicate untranslated regions and black lines indicate introns (i). Colored bars denote Exons (E). (B) CCN2/CTGF protein and protease cleavage sites with four distinct modules; IGFBP, Insulin-like growth factor binding protein; VWF-C/CR, von Willebrand factor type C/chordin-like cystein-rich; TSP1, thrombospondin 1; CT, carboxy terminal [102].

CCN2 is the most studied member of the CCN family in the cardiovascular system. CCN2 may play a vital role in cardiac remodeling because of its consistent up-regulation in models of cardiac injury, hypertrophy, and fibrosis and its profound effects on cardiomyocytes, fibroblasts, and endothelial cells [103, 104]. Our group demonstrated that CCN2 increases the tolerance of the heart towards ischemia/reperfusion injury as well as to cardiomycytes towards hypoxia/reoxygenation injury [105]. Our group also demonstrated that Angiotensin-II-induced myocardial CCN2 contributes to myocardial remodeling in heart failure mediated via Angiotensin-II type 1 (AT_1) receptors situated on cardiac fibroblasts [106].

1.7 Wnt1-inducible Signaling Pathway 2 (WISP-2) or CCN5

CCN5 is a unique member of the CCN family of genes [107]. All other CCN proteins contain four distinct domains: (i) insulin-like growth factor-binding domain (IGFBD), (ii) von Willebrand factor type-C (vWC), (iii) thrombospondin type-1 (TPS-1), and (iv) C-terminal domain (CT), whereas CCN5 lacks the CT domain (Fig 1.6). It has been demonstrated that the CT domain regulates the proliferative activity of CCN1 and CCN2 and lacking this CT domain in CCN5 may contribute to its converse effects compared to CCN1 and CCN2 [108-110]. Yoon et al. demonstrated that over-expressed CCN5 inhibits cardiac hypertrophy and fibrosis by blocking the TGF-β-SMAD signaling pathway in response to pathological stimuli both *in vitro* and *in vivo* [111].

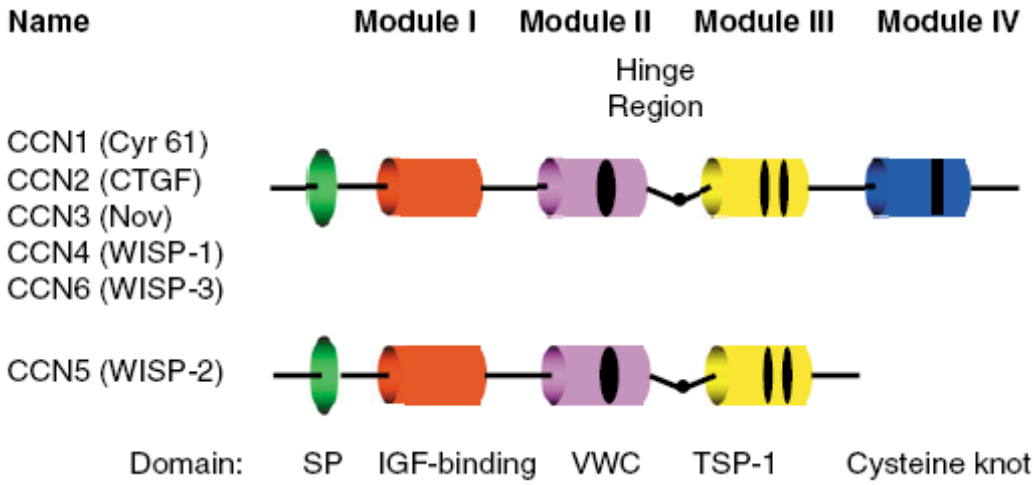

Figure 1.6 Structure of CCN family members. The CCN family members, CCN1 (Cyr61), CCN2 (CTGF), CCN3 (nov), CCN4 (WISP-1), CCN5 (WISP-2) and CCN6 (WISP-3), whereas CCN5 differs from other CCN proteins by lacking CT domain [112].

1.8 Growth Differentiation Factor 15 (GDF15)

Growth differentiation factor 15 (GDF15) is a member of the transforming growth factor β (TGF-β) superfamily; is a secreted macrophage inhibitory cytokine mainly expressed by activated macrophages by inflammatory stimuli. Normally, expression of GDF15 is abundant in the placenta and the prostate, but not in many other organs, including the heart. However, IL-1, TNF-α and TGF-β in macrophages induce GDF15 expression rapidly, thereby modulating macrophage activation and inflammation. p53, a tumor suppressor protein, also induces GDF15 expression and acts as a growth inhibitory molecule in tumor cells [113-115].

Kemph et al demonstrated that over-expression of GDF15 in cardiomyocytes increases the tolerance of the heart towards ischemia/reperfusion (I/R) via the nitric oxide-peroxynitrite dependent signaling pathway [116]. Xian Su et al. also demonstrated that GDF15 plays a role as a novel anti-hypertrophic factor in the heart through a mechanism involving SMAD protein [117]. Our group also demonstrated that cardiomyotes of CNN2 over-expressing transgenic mice increased expression of GDF15 significantly which may constitute an autocrine loop that activates SMAD2 protein and inhibits cardiac myocyte growth [105].

2. AIM OF THE STUDY

The purpose of the study was to investigate how LPS regulates the expression of TNF-α, IL-1β, CCN2, CCN5 and GDF15 in adult cardiac myocytes and cardiac fibroblasts. In addition, it would also be interesting whether LPS results in cell death in adult mouse cardiac myocytes. Aims of study are given below elaborately.

- ✓ To isolate adult mouse cardiac myocytes and cardiac fibroblasts.
- ✓ To maintain adult mouse cardiac myocytes and cardiac fibroblasts cell cultures *in vitro*.
- ✓ To investigate the effects of LPS on the adult mouse cardiac myocytes and fibroblasts.
- ✓ To study the effects of LPS on the regulation of mRNA levels of TNF-α and IL-1β in adult mouse cardiac myocytes and fibroblasts.
- ✓ To study the effects of LPS on the regulation of mRNA levels of CCN2, CCN5 and GDF15 in adult mouse cardiac myocytes and fibroblasts.
- ✓ To study the effects of LPS on the regulation of protein levels of TNF-α and IL-1β in adult Mouse cardiac myocytes and fibroblasts.
- ✓ To study the effects of LPS on regulation of protein levels of CCN2, CCN5 and GDF15 in adult mouse cardiac myocytes and fibroblasts.
- ✓ To study the effects of LPS on the viability of adult mouse cardiac myocytes.

3. MATERIALS

3.1 Isolation of Adult Mouse Cardiac Myocytes and Fibroblasts

Chemicals	Suppliers
MEM (Minimum Essential Medium) with glutamine	Gibco
DMEM (Dulbecco's Modified EagleMediu)	Gibco
Calf Serum	HyClone
Fetal Calf Serum	Sigma
Gentamycin	Sanofi Aventis
Bovine serum albumin (endotoxin and lipid free)	Sigma
CaCl2 (1 M)	Sigma
BDM (2.3-Butanedione monoxime; 500 mM)	Sigma
Penicillin-G	Sigma
Na-ATP (200 mM)	Sigma
Laminin	Invitrogen

Equipments	Suppliers
Steri Cycle CO_2 Incubator	Thermo Scintific
Perfusion System	Watson Marlow
Laminar flow culture hood	Holten
Surgery scissors	Aesculap

Solutions	Amount
Perfusion Buffer (1L)	
NaCl	120 mM
KCl	14.75 mM
KH_2PO4	0.6 mM
Na_2HPO_4 $2H_2$	0.589 mM
$MgSO_4$ $7H_20$	1.22 mM
$NaHCO_3$	4.64 mM

Taurine.....29.98 mM

BDM.....9.89 mM

Glucose.....5.55 mM

Na-HEPES.....10 mM

dH_2O……..Up to 1L

Digestion Buffer (50ml)

Perfusion buffer.....50 ml

Collagenase 2.....120 mg

Stopping Buffer (20 ml)

Perfusion buffer.....18 ml

Calf Serum.....2 ml

$CaCl_2$ (100 mM).....2.5 µl

Stopping Buffer for Ca-introduction (30 ml)

Perfusion buffer.....27 ml

Calf Serum.....3 ml

A) 10 µl of 100 mM $CaCl_2$ in 10 ml Stopping Buffer.

B) 40 µl of 100 mM $CaCl_2$ in 10 ml Stopping Buffer.

C) 90 µl of 100 mM $CaCl_2$ in 10 ml Stopping Buffer

Myocyte Plating Medium

MEM with HBS.....42.5 ml

Penicillin.....0.5 ml

BDM.....1 ml

ATP.....0.5 ml

Calf Serum.....5 ml

Myocyte Long-Term Culture Medium

MEM with HBSS.....48.5 ml

Penicillin.....0.5 ml

BDM.....1 ml

BSA.....0.5 ml

3.2 RNA Isolation

Chemicals	Suppliers

RNeasy® Mini Kit.....Qiagen
β-mercaptoethanol.....Sigma
TRIzol® Reagent……Invitrogen
Chloroform…….Sigma
Glycogen……..Invitrogen

Equipments	Suppliers

Centrifuge and rotor capable of reaching up to 12000xg……Biofuge
Heating Block……...Techne
ND1000 Spectrophotometer……NanoDrop

3.3 Reverse Transcription

Chemicals	Suppliers

TaqMan Reverse Transcription Reagents……Applied Biosystems

Equipments	Suppliers

Thermo Cycler…….Applied Biosystems

3.4 TaqMan Real-Time PCR

Chemicals	Suppliers

TaqMan Real-Time PCR amplification

Taqman 2x PCR master mix.....Applied Biosystems
Taqman gene expression assays (20x)…….Applied Biosystems

a) CTGF (Mm01192933_g1)

b) WISP-2 (Mm00497471_m1)
c) GDF-15 (Mm00442228-m1)
d) TNF-α (Mm00443260_g1)
e) IL-1β (Mm00434228_m1)

Equipments	Suppliers

TaqMan Real-Time PCR amplification

MicroAmp™ Optical 96-well reaction plate……...Applied Biosystems
MicroAmp™ Clear Adhesive Film……..Applied Biosystems
7900HT Real-Time PCR Machine……...Applied Biosystems
Sequence Detection Sytem (SDS) 2.2 software……...Applied Biosystems
Microsoft Excel 2007……...Microsoft
GraphPad Prism version 4……GraphPad

3.5 Western Blot Analysis

Chemicals	Suppliers

30% Acrylamide/Bis Solution, 37.5:1……Bio-Rad
Trizma Base……...Sigma
Glycine……...Sigma
Glycerol……..Sigma
SDS……..Invitrogen
MiliQ H_20.....MiliPore
AmmoniumPersulfate.....Sigma
TEMED……..Sigma
Methanol……Sigma
PVDF Transfer Membrane……..GE HealthCare
Whatman Paper……...Bio-Rad
Nonfat Dry Milk……Bio-Rad
Casein……..Thermo Scientific
10x PBS……..Lonza

10x TBS……..Lonza

Tween-20 Detergent……...Sigma

LumiGlo……KPL

Primary Antibodies

IL-1β (Catalog No: 8689)……..Cell Signaling

TNF-α (Catalog No: 3707)……Cell Signaling

CCN2 (Catalog No: Sc-14939)……...Santa Cruz

CCN5 (Catalog No: Sc-8868)……Santa Cruz

GDF15 (Catalog No: ABIN372779)……...Antibodies-online

Secondary Antibodies

Anti-rabbit IgG HRP……GE HealthCare

Anti-goat IgG HRP…….Santa Cruz

Solutions	Amont

Lysis Buffer (4ml)

SDS (10 %)……400 µl

Tris-HCl (1M; pH 7.4)……40 µl

dH_2O……Up to 4 ml

12% Separating Gel (15 ml)

dH_2O……...4.9 ml

Acrylamide Mix (30%)……6 ml

Tris base (1.5; pH 8.8)……...3.8 ml

SDS (10%)…….0.150 ml

Ammonium Persulfate (10%)……0.150 ml

TEMED……..0.006 ml

5% Stacking Gel (5 ml)

dH_2O……...3.4 ml

30% Acrylamide Mix…….0.830 ml

1.5 Tris base (pH 6.8)…….0.630 ml

10% SDS……0.050 ml

10% Ammonium Persulfate……...0.050 ml

TEMED……..0.005 ml

2x Loading Buffer (100ml)

Tris HCl pH 6.8……..125 mM
SDS……4%
Glycerol……10%
Bromophenol Blue……...0.1%
β-Mercaptoethanol……100 µl
dH_2O……Up to 100 ml

5x Running Buffer (1L)

Tris Base……15 g

Glycine……..72 g

SDS……5 g

dH_2O……Up to 1L

10x Blotting Buffer (1L)

Tris Base……30.3 g

Glycine……144 g

dH_2O……..Up to 1L

Blotting Buffer (1L)

10x Blotting Buffer ……..100 ml

Methanol……...200 ml

dH_2O……Up to 1L

10xPBS (Ph 7.4) Buffer

NaCl……..80 g

KCl……...2.0 g

Na_2HPO_4……14.4 g

KH2PO4……...2.4 g

dH_2O……..Up to 1L

10x TBS (pH 7.4) Buffer

Trisbase.....30 g

NaCl.....88 g

KCl.....2 g

dH_2O……..Up to 1L

PBST Buffer (1L)

10x PBS…….100 ml

Tween 20 detergent……...1 ml

dH_2O……..Up to 1L

TBST Buffer (1L)

10x TBS……100 ml

Tween 20 detergent……...1 ml

dH_2O……..Up to 1L

Blocking Buffer (6ml)

5% Milk Buffer in PBST or TBST

5% Casein Buffer in PBST

Equipments	**Suppliers**

Ultrasonic Cell Disrupter…….Microsom

ELISA Reader Machine…….Victor

Gel Electrophoresis Apparatus……...Bio-Rad

Electronic Transfer Apparatus……Bio-Rad

Chemiluminescence Apparatus…….Kodak

3.6 Cell Viability Test

Chemicals	Suppliers
Trypan Blue	Sigma

Equipments	Suppliers
0.45 µm non-pyrogenic Filter	Milipore
Light Microscope	Leica Microsystems

4. METHODS

4.1 Isolation of Adult Mouse Cardiac Myocytes and Cardiac Fibroblasts

Isolation of cardiac myocytes or fibroblasts was performed according to the protocol published by Timothy D. O'Connel with minor modifications [118].

4.1.1 Excision and Cannulation of the Heart

The mouse was anesthetized with the isoflurane. The anesthetized mouse was injected intraperitoneally with 0.5 ml heparin (100 IU/ml in phosphate buffered saline (PBS)). After few minutes, the chest was wiped with 70% ethanol and opened with small scissors. Forceps were used to peel the rib cage to expose the heart. The heart was lifted gently with forceps, the pulmonary vessels were identified, and the aorta was cut between the carotid arteries. The excised heart was placed immediately in a 60 mm dish containing 10 ml of perfusion buffer. Extraneous tissue was removed, and the heart was transferred to a new 60 mm dish with perfusion buffer. The heart was cannulated using fine-tip forceps to slide the aorta onto the cannula under magnification so that the cannula was above the aortic valve. The aorta was tied to the cannula with 6/0 silk thread and perfusion was started immediately. Total time to cannulate the heart was less than one minute.

4.1.2 Perfusion and Enzymatic Digestion of the Heart

After cannulation, the heart was perfused with perfusion buffer for 4 minutes at a flow rate of 4 ml/min to flash blood and extracelluar calcium from the vasculature (Removal of calcium to stop contraction). After 4 minutes, perfusion buffer was replaced with myocyte digestion buffer and the heart was perfused for 3 minutes at a flow rate of 4 ml/min. Myocyte digestion buffer was collected and discarded. 15 µl of 100 mM $CaCl_2$ was added to the myocyte digestion buffer in the reservoir and continued to perfuse the heart for 8 minutes at a flow rate of 4 ml/min. The total digestion time was about 11 minutes. After enzymatic digestion, the heart became swollen and slightly pale.

4.1.3 Myocyte Dissociation

Once enzymatic digestion of the heart was completed, it was cut from the cannula just below the atria using sterile fine scissors. The ventricles were placed in sterile 60-mm Valmark dish containing 2.5 ml of myocyte digestion buffer. From this point forward all the steps were performed under a laminar flow culture hood using sterile technique. The ventricles were teased into 10 to 12 pieces with fine tip forceps, and 5 ml of myocyte stopping buffer was added to the dish. The digested tissue was gently pipetted up and down several times through a sterile plastic transfer pipette. The cell suspension was transferred to a 15-ml polypropylene conical tube. The plate was rinsed with 2.5 ml of myocyte stopping buffer and combined with the cell suspension to a final volume of 10 ml. The digested heart tissue was further dissociated, using sterile plastic transfer pipettes until all the large pieces of the heart tissue were dispersed in the cell suspension. The myocytes were allowed to sediment by gravity for a few minutes in 15-ml tube. The tube was centrifuged for 3 minutes at 300 rpm. The pellet was resuspended gently in 10 ml myocyte stopping buffer, and the supernatant containing non-myocytes was transferred to a 50 ml tube for cardiac fibroblasts preparation.

4.1.4 Calcium Re-introduction

Three 15 ml tubes containing 10 ml myocyte stopping buffer with following calcium concentration were prepared.

1) 100 µM calcium (10 µl of 100 mM $CaCl_2$ in 10 ml Myocyte Stopping Buffer)
2) 400 µM calcium (40 µl of 100 mM $CaCl_2$ in 10 ml Myocyte Stopping Buffer)
3) 900 µM calcium (90 µl of 100 mM $CaCl_2$ in 10 ml Myocyte Stopping Buffer)

A three-step calcium reintroduction to myocytes was performed as follows. The myocytes were centrifuged for 3 min at 300 rpm. The supernatant was removed, and the pellet was resuspended with 10 ml of myocytes stopping buffer from tube 1. The above steps were repeated with myocyte stopping buffer from tube 2 and 3 containing 400 µM and 900 µM calcium respectively. Finally, the pellet was resuspended with myocyte plating medium and cells were incubated at 37°C containing 1.2 mM of calcium.

4.1.5 Culture of Cardiac Myocytes

The myocytes were platted on the laminin coated 6 well dishes. The plates were incubated in a 2.5% CO_2 at 37°C and cells were allowed to attach. After two hours the medium was aspirated and cell debris was removed by washing with 2 ml of myocyte plating medium. 2 ml of myocyte plating medium was added to each well and plates were transferred to the

incubator. Approximately 80% cells were found to be rod shaped. The cells were retained in myocyte plating medium over night and were treated with LPS or were used for cell viability assay. Fig 4.1 shows a photomicrograph of adult mouse cardiac myocytes plated on laminin coated plate.

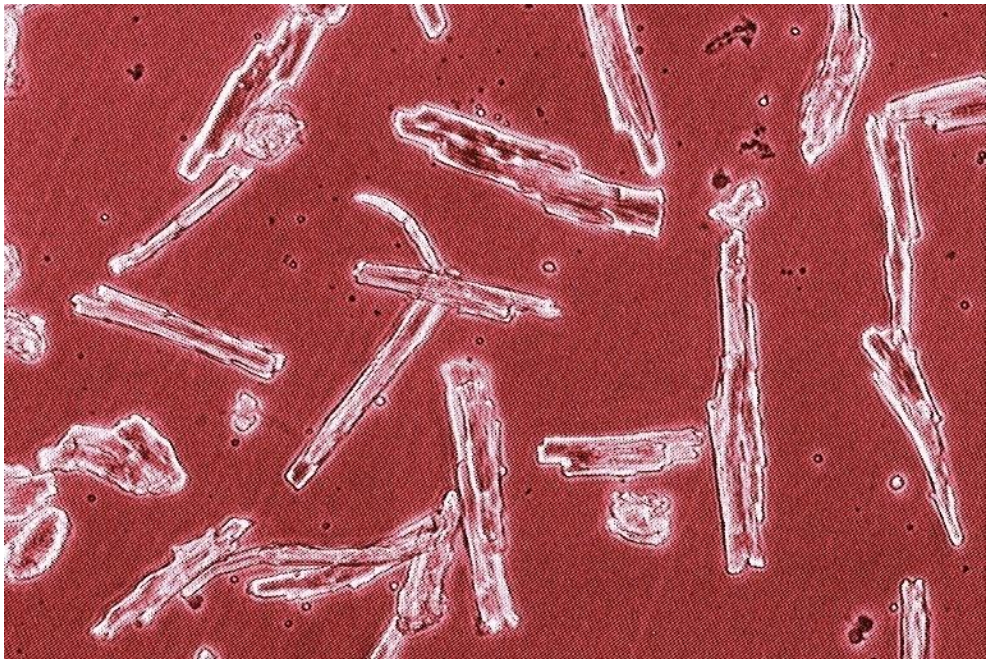

Figure 4.1 Adult mouse primary cardiac myocytes after plating on laminin coated dishes containing myocyte plating medium.

4.1.6 Preparation of Cardiac Fibroblast

Mouse cardiac fibroblasts were obtained from the hearts by differential centrifugation of cardiac cells released after enzymatic digestion of the hearts as mentioned in section 3.1.3. Supernatants containing non-myocytes from 2-3 hearts were pooled and centrifuged at 1800 g for 5 minutes.

The supernatant was discarded, and the pellet was mixed in 10 ml of growth medium (DMEM) containing 10% Fetal Calf Serum and Gentamicin (28 µg). The cell suspension was transferred to a 100 mm non-coated cell culture dish, and the cell culture dish was transferred to humidified incubator with 5% CO_2 at 37°C. After 2 hours the medium was aspirated, and the cell culture dish was washed with fresh growth medium (DMEM) to remove the unattached cells. The attached cells (cardiac fibroblast) were maintained and propagated in growth medium (DMEM) (Fig. 4.2). Cells were split at 100% confluency and plated into 6 well plates for further experiment.

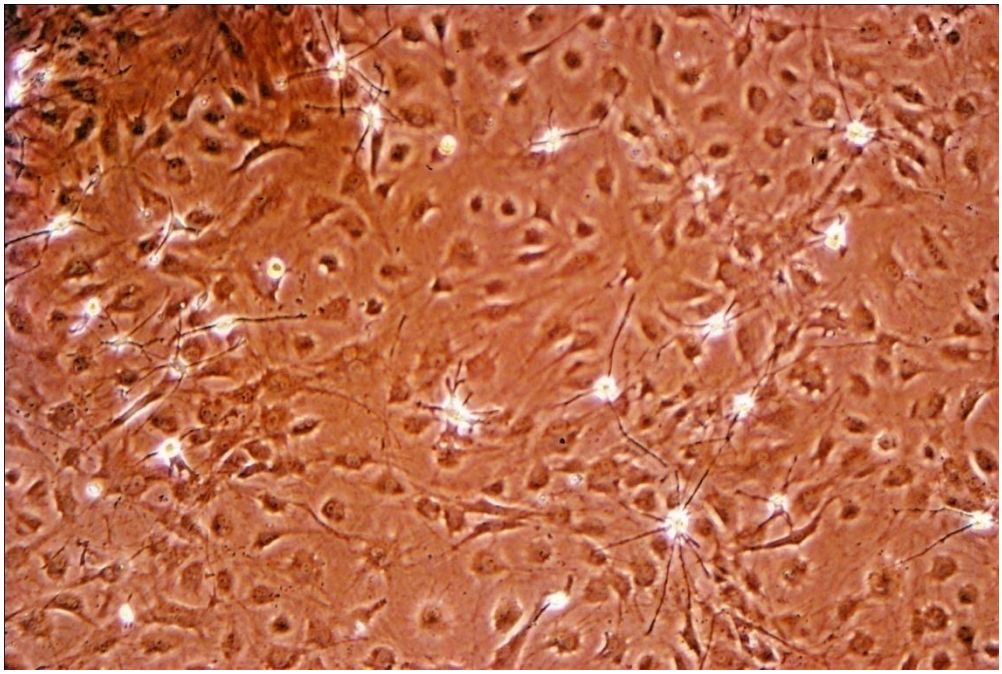

Figure 4.2 Mouse primary cardiac fibroblasts after 100% confluency

4.2 Assay of mRNA Expression Levels

General reference: www.appliedbiosystems.com

Real-time quantitative PCR (qPCR) was used to investigate the mRNA expression levels of five target genes in LPS treated mouse cardiac fibroblasts and cardiac myocytes. Real-Time qPCR is an advanced PCR technique that can amplify and simultaneously quantify a targeted DNA molecule. In real-time PCR, DNA amplification is detected in "real- time" during early phases of PCR when the PCR product increases exponentially (Fig. 4.3).

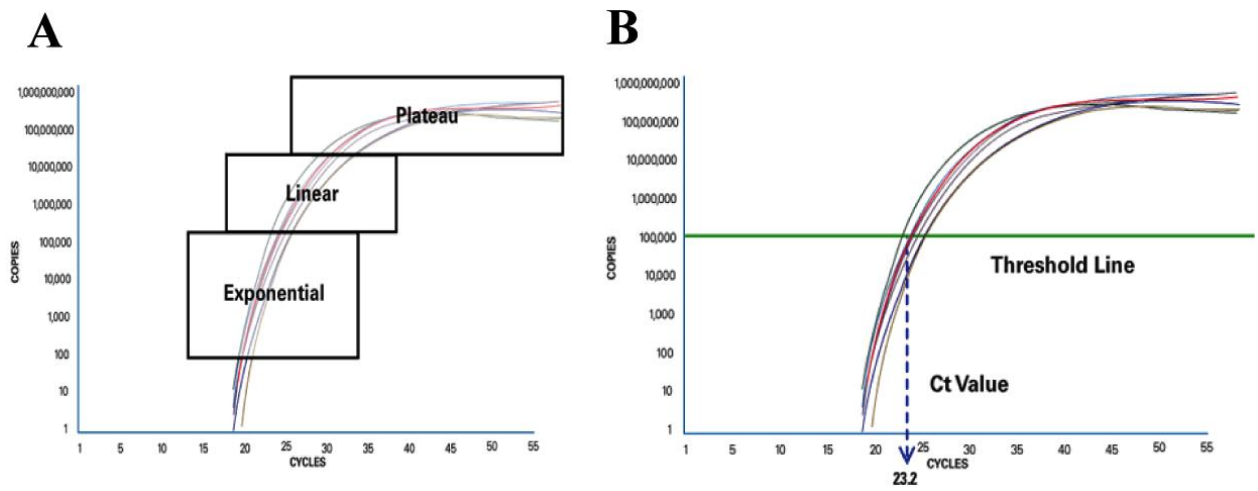

Figure 4.3 In Real-Time PCR, the exponential phase gives off the most precise and accurate data for quantification (Fig A). The PCR cycle at which the sample reaches a fluorescent intensity above background is called the Cycle Threshold (Ct) (Fig B). The Ct value is used to quantify the expression levels of the target gene. By comparing the Ct values of samples of unknown concentration with a series of standards, the amount of template DNA in an unknown reaction can be accurately determined (www.appliedbiosystems.com).

To assess mRNA expression levels of five target genes in LPS treated cardiac cells by real time qPCR, total RNA was extracted from the treated and non-treated cells. The mRNA was reverse- transcribed using the TaqMan Reverse Transcription Reagent Kit and subsequently real-time qPCR of each sample was run in triplicates using TaqMan Pre-developed Assay Reagents (TaqMan PDARs) and ABI Prism 7900 Sequence Detection System and Software (Applied Biosystems). TaqMan PDARs consists of a forward primer, a reverse primer and an oligonucleotide probe designed to amplify specific target sequences in cDNA samples using the 5´ nuclease activity. The oligonucleotide (Taqman probe) probe is dual labeled and comprises a reporter dye for example, 6-carboxy fluorescin (FAM) dye linked to the 5´ end of the probe, a nonfluorescent quencher (NFQ) at the 3´ end of the probe.

For quantitation of gene expression in real-time PCR, relative standard curve method (relative quatitation) was applied. Relative standard curve method quantifies differences in the expression levels of target gens between treated and non-treated samples. The data output is expressed as a fold-change or a fold-difference of expression levels. A relative standard curve method is used to quantify expression of both target gene and housekeeping gene. To generate a standard curve a dilution series of RT-reaction is made and run for both the target and the endogenous control gene. However, to assay mRNA expression levels of the genes by real time qPCR, the entire procedure is described as follows.

4.2.1 RNA Isolation

General reference: www.qiagen.com & www.invitrogen.com

Total RNA was extracted from cardiac fibroblasts by using Qiagen RNeasy Mini Kit, whereas RNA from cardiac myocytes was isolated by using both Qiagen RNeasy Mini Kit and TRIzol® reagent. The TRIzol® reagent, a mono-phasic solution of phenol and guanidine isothiocyanate is known to maintain the integrity of RNA based on the principle of phase separation. TRIzol® reagent method involves sample homogenization with TRIzol® reagent, phase separation and precipitation of RNA. The eluted RNA from Qiagen spin column and RNA obtained from TRIzol® reagent method were stored at -80°C until further use.

4.2.1.1 RNA Isolation from Cardiac Fibroblasts

Cardiac fibroblasts were seeded at a density of $3x10^5$ cells/well using 6 well plates. Next day, the cells were incubated with and without LPS in a humidified chamber at 37°C for 3 hours. After stimulation with LPS, the medium was aspirated and cells were washed with (2 ml/well) saline water and were immediately lysed by adding 350 µl of lysis buffer. The cell lysates were transferred to eppendorf tube and were further homogenized using 25G needle. 70% ethanol (350 µl) was added to cell lysates. Cell lysates were transferred to RNA spin column. RNA was eluted with elution buffer. RNA concentration was measured using Nano-Drop spectrophotometer and then RNA was stored at -80°C until further use.

4.2.1.2 RNA Isolation from Cardiac Myocytes

For cardiac myocytes Qiagen RNA spin column method was not able to produce desirable concentration of RNA. Therefore, TRIzol® reagent method was used to get required amount of RNA. After washing, 1ml of TRIzol® reagent was immediately added to each well. The cells were lysed by pipetting up and down several times and were proceeded to phase separation. The homogenized samples were incubated for 5 minutes at room temperature to permit complete dissociation of the nucleoprotein complex and 0.2 mL of chloroform was added. The tubes were shaken vigorously and were incubated for 2–3 minutes at room temperature. The samples were centrifuged at 12,000 × g for 15 minutes at 4°C and the aqueous phase of the samples was transferred into a new tube and proceeded to the RNA isolation procedure. Then, as a carrier, RNase-free glycogen (7 µg) was added to the aqueous RNA solution. To precipitate RNA, 100% isopropanol (0.5 ml) was added and tubes were incubated at room temperature for 10 minutes. To pellet the precipitated RNA, the tubes were

centrifuged at 12,000 × g for 10 minutes at 4°C and the pellet was washed with 1 ml of 75% ethanol. The tubes were vortexed briefly and centrifuged at 7500 × g for 5 minutes at 4°C. Supernatant was discarded and RNA pellet was air dried for 5–10 minutes at room temperature. The RNA pellet was resuspended in RNase-free water and incubated in a heating block at 55°C for 10–15 minutes. The RNA concentration was determined using Nano-Drop spectrophotometer and RNA was stored at -80°C until further use.

4.2.2 Reverse Transcription

Reverse transcription (RT) is a process in which single stranded RNA is transcribed into complementary DNA (cDNA) by Reverse Transcriptase Enzyme (RNA-dependent DNA polymerase). The extremely unstable nature of RNA has made the cDNA popular for a wide variety of experimental purposes; from determining the level of gene expression for a few genes to large-scale screening among different biological systems. In 1970s Howard Temin and David Baltimore discovered Reverse Transcriptase enzyme independently [119].

A RT-reaction requires RNA, a primer and reverse transcriptase. In this reaction, three types of primers can be used; oligo (dT) primers, random (hexamer) primers or gene specific primers depending upon subsequent analysis. In this study, RT-reactions were carried out by using random (hexamer) primers supplied in TaqMan Reverse Transcription Reagents Kit (Applied Biosystems). After quantification, the concentration of RNA was adjusted to 50 ng/µl in all the samples. Each RT-reaction was carried out in a total volume of 50 µl. For cardiac fibroblasts, 100 ng of total RNA was used in an RT reaction (50µl), whereas for cardiac myocytes 500 ng of total RNA was reversed transcribed. A basic RT-reaction includes following.

Reagents	Volume (µl)
10x RT-buffer	5
MgCl2 (25 mM)	11
dNTP (10 mM)	10
Hexamers (50 mM)	2,5
Rnasin (20 U/µl)	1
MultiScribe RT (50 U/µl)	1,25
H_2O	17,25
RNA (100 ng)	2
Total	50

The RT reaction mixtures were incubated in thermal cycler 2720 (Applied Biosystems). The thermal cycler 2720 was programmed as follows.

Table Conditions for RT reaction

	Step 1	Step 2	Step 3	Step 4
Temperature(°C)	25	48	95	4
Time	10 min	30 min	5 sec	∞

The cDNA samples were stored at -20°C until further use.

4.2.3 TaqMan® Real-Time PCR amplification

Real-time quantitative PCR (qPCR) of each sample was run in triplicates in 96 wells plates using TaqMan Pre-Developed Assay Reagents, the ABI Prism 7900 Sequence Detection System and software (Applied Biosystems, Foster City, CA, USA) according to the manufacturer's instructions. A standard curve was obtained from 2-fold serial dilutions of cDNA, obtained from reverse transcription of total RNA either from cardiac fibroblasts or cardiac myocytes. For all specific mRNA amplified, linear inverse correlations were observed between the amount of mRNA and C_T value (number of cycles at threshold lines). Gene expression was presented relative to the levels of 18S rRNA or Glyceraldehyde 3-phosphate dehydrogenase (GAPDH) as the housekeeping genes. A basic TaqMan Real-Time PCR reaction includes the following

Reagents	**Volume (μl)**
Tagman Master Mix (2x)	40
Taqman gene expression assay (20x)	4
H_2O	31
cDNA from RT-reaction	5
TOTAL	80

After adding 5 μl of cDNA, the tubes were vortexed and 25 μl of PCR mix per well was added to 96 wells plate (Applied Biosystems). MicroAmp™ Clear Adhesive Film was used to seal the plates before placing in 7900HT Real-Time PCR System. 7900HT Real-Time PCR System uses standard conditions for PCR amplification reaction. The Conditions for PCR amplification reactions in a 7900HT Real-Time PCR System are listed in the following table.

	Hold	Hold	Cycles(40 cycles)	
Temperature	50°C	95°C	95°C	60°C
Time	2 min	10 min	15 sec	1 min

4.2.4 Data Analysis

Results from the 7900HT Real-Time PCR System were obtained as Sequence Detection Sytem (SDS) 7900HT documents, which were imported to Microsoft Excel, (Microsoft Corporation, USA, version 2007). Quantification of the expression levels of genes in LPS stimulated and control mouse cardiac fibroblasts and cardiac myocytes samples was performed by a standard curve method. Gene expression was presented relative to the levels of 18S rRNA or GAPDH as follows.

$$\text{Normalization of gene A} = \frac{\text{Expression of gene A}}{\text{Expression of Human 18S rRNA or Mouse GAPDH}}$$

Normalization and other statistical analysis of data were performed by using Microsoft Excel 2007 and GraphPad Prism version 4.

4.3 Western Blot Analysis

Western blotting is a powerful and well-known tool to detect and quantify a protein of interest in a complex mixture [120]. The technique detects protein samples immobilized on a nitrocellulose or polyvinylidene fluoride (PVDF) membrane. There are two types of Western blotting techniques i.e. direct and indirect Western blotting. The direct Western blotting involves a reporter-labeled primary antibody that directly binds to the target protein, whereas the indirect detection involves a labeled secondary antibody [121] that binds to a non-labeled primary antibody (Fig. 4.4). Direct Western blot analysis takes less time than the indirect since further incubation with a secondary antibody is not necessary in direct Western blotting. In addition, background signal due to cross-reactivity of secondary antibody can also be avoided in direct technique [122].

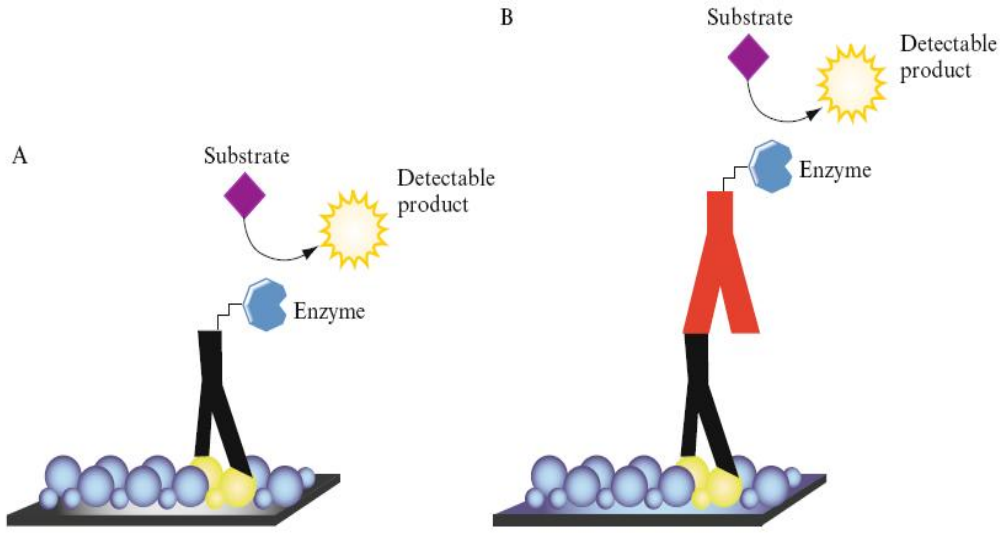

Figure 4.4 Direct (A) and indirect (B) western blotting methods. In panel A, labeled primary antibody creates a detectable signal by binding to antigen on the membrane and reacting with the substrate. In panel B, unlabeled primary antibody binds to the antigen and a labeled secondary antibody binds to that primary antibody to react with the substrate [123].

The direct method generally shows less sensitivity than indirect detection method and is preferably used only when the target is relatively abundant. A conventional indirect Western blot that was used in the experiment begins with resolving of protein samples by sodium dodecyl sulfate polyacrylamide gel electrophoresis (SDS–PAGE) and then electrophoretically transferring to the membrane. After blocking, the membrane is incubated with a primary antibody (poly- or monoclonal). The membrane is then washed and incubated with an enzyme-conjugated secondary antibody that has specific affinity for primary antibody. After

washing again, the membrane is incubated with an appropriate enzyme substrate. The signal is either visually detected, if a colorimetric substrate was used, or is detected with X-ray film or chemiluminescence/fluorescence signals which are recorded by using digital imaging system. The remarkable advances in Western blotting have been made and now, highly sensitive-enhanced chemiluminescent substrates, imaging systems and, a wide variety of photostable fluorophores are commercially available. The widespread use of extremely sensitive chemiluminescent substrates [124, 125] has resulted in nearly avoiding the use of radioisotope-labeled probes. Protein A or G labeled with ^{125}I was once commonly used as a secondary detection reagent; however, the enhanced chemiluminescent substrates can detect proteins down to the low-femtogram level with high signal-to-noise ratios [123]. In this study, Western blot analyses of target proteins were performed as follows.

4.3.1 Cell preparation

Protein lysates were prepared from LPS stimulated and control mouse cardiac fibroblasts and cardiac myocytes. After stimulation with LPS (1 μg/ml) for 3 , 6 and 24 hours at 37°C the cells were washed with saline water and were lysed with protein lysis buffer containing 10% SDS and 10 mM Tris-HCl (pH 7.4). The samples were homogenized by sonication and then assayed for protein concentration. Samples were denatured by heating at 100°C in Laemmli's buffer. Heating denatures the proteins, unfolding them completely. The SDS surrounds the protein with a negative charge and the β-mercaptoethanol inhibits the reformation of disulfide bonds.

4.3.2 Gel electrophoresis and electroblotting

In gel electrophoresis, the proteins are separated based on their molecular weight. The polyacrylamide gel which was used in this study consists of 12% separating gel and 5% stacking gel. Samples (20 μg) were loaded in each lane of the gel and protein samples were run at 25 mA through the stacking gel and thereafter at 50 mA through the separating gel. Proteins were separated based on their molecular weight into bands within each lane under the wells. One lane was loaded with molecular weight standards, a commercially available mixture of proteins with known molecular weights (Bio-Rad). After electrophoresis, the separated proteins were electro-transferred from gel to PVDF membrane according to manufacturer’s instructions. Briefly, the methanol activated membrane was placed face-to-face with the gel in a sandwich and the sandwich was placed in blotting buffer. Then current

was applied to initiate the transfer. The charged proteins moved from the gel onto the PVDF membrane.

4.3.4 Membrane blocking and antibody incubation

Blocking of membrane with blocking buffer prevents the non-specific interactions between membrane and antibodies being used for detection of the target proteins. After electro-blotting, the membrane was briefly washed with PBS or TBS. For blocking, the membrane was incubated in blocking buffer (5% non-fat dry milk or 5% casein in TBST or PBST, respectively) for one hour at room temperature. After washing three times for 5 minutes each with appropriate washing buffer, the membranes were incubated with primary antibody in primary antibody dilution buffer with gentle agitation overnight at 4°C. The membrane was washed three times for 5 minutes each and incubated with horseradish peroxidase (HRP) conjugated species appropriate secondary antibody for one hour at room temperature. The unbound secondary antibody was washed and preceded to detection step. For detection of the target proteins, the membranes were incubated with 6 ml LumiGLO with gentle agitation for 1 minute at room temperature. The signals were recorded by using KODAK Image Station 4000R Digital Imaging System and KODAK Molecular Imaging Software. Finally, expression levels of target proteins were determined by densitometric analysis using KODAK Molecular Imaging Software.

4.4 Cell Viability

The trypan blue exclusion assay is performed to determine the number of viable cells in a given cell culture. The test is based on the principle that live cells exclude trypan blue, whereas dead cells stain with trypan blue. To perform the test, cell suspension is simply mixed with dye and is visually examined to determine whether cells take up or exclude the dye.

In this study, trypan blue exclusion assay was performed to evaluate the cell viability of LPS stimulated and control primary mouse cardiac myocytes. After isolation, the cardiac myocytes were plated in 6 wells plates and kept in a humidified chamber overnight at 37°C. Before treatment with LPS, the dead cells were removed and the fresh culture medium was added to each well. For viability test, the cells were incubated in the absence and presence of LPS (0.1μg/ml and 10μg/ml) and cell viability was determined at four different time points

after stimulation. To count the number of dead cells, 50 µl of filtered trypan blue was added to each well, waited for two minutes to stain the dead cells. Total cells including dead and viable cells were counted and percentage of viable cells was determined. Statistical analyses were performed by using Graph Pad Software (Graph Pad Prism 4.0).

4.5 Statistical Analysis

All the data were given as means ±SE. Two tailed Student's t-test was applied for statistical comparisons of two groups, whereas one-way ANOVA and two-way ANOVA with Bonferroni's test were performed for the comparison of multiple groups. P values <0.05 were considered to be statistically significant.

5. RESULT

5.1. Expression of TNF-α and IL-1β mRNA in LPS Stimulated Cardiac Fibroblasts and Cardiac Myocytes

To investigate the effects of LPS on mRNA expressions of TNF-α and IL-1β, adult mouse cardiac fibroblasts and cardiac myocytes were stimulated for 3 hours with increasing concentrations of LPS as indicated in Fig. 5.1 and 5.2. As shown in Fig. 5.1, real-time quantitative PCR (qPCR) analysis revealed robust induction of TNF-α and IL-1β mRNA expressions in LPS (1µg/ml) stimulated cardiac fibroblasts and cardiac myocytes. The mRNA expression levels of TNF-α and IL-1β in cardiac fibroblasts were up-regulated 20 fold ($P<0.05$; Fig. 5.1A) and 23 fold ($P<0.05$; Fig. 5.1B) respectively, whereas in cardiac myocytes TNF-α mRNA expression levels were elevated 10 fold ($P<0.0001$; Fig. 5.1C) and that of IL-1β were increased 5 fold ($P<0.0001$; Fig. 5.1D) above the control levels (non-stimulated). In addition, we investigated the concentration dependent effects of LPS on the mRNA levels of the two cytokines in primary cardiac cells.

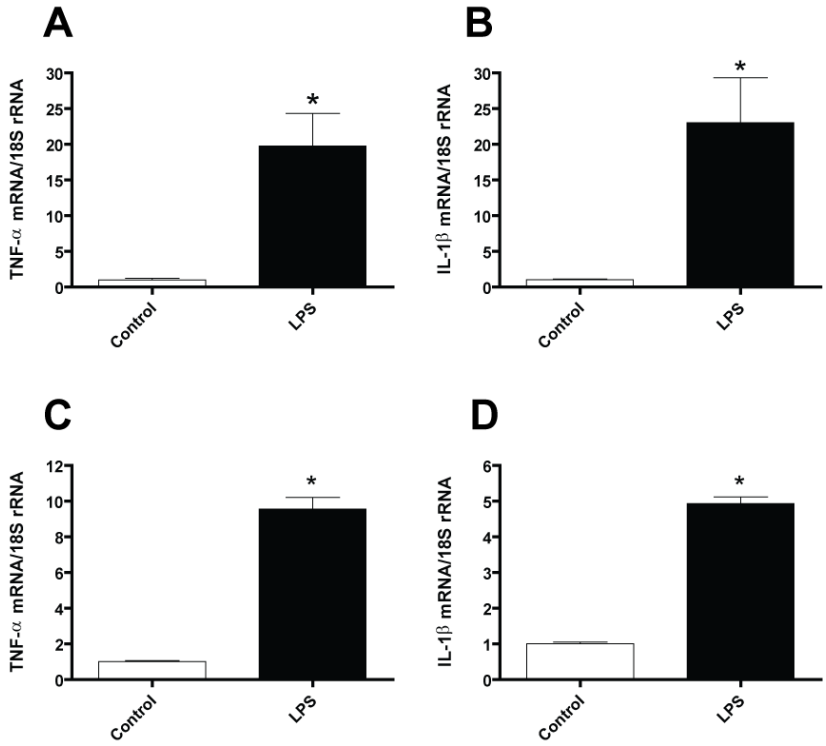

Figure 5.1 Real-time qPCR analysis demonstrating mRNA levels of TNF-α and IL-1β in adult mouse cardiac fibroblasts **(A and B)** and myocytes **(C and D)** incubated in the absence or presence of LPS (1 µg/ml ; 3 hours). Data are presented as ratios of TNF-α or IL-1β mRNA levels relative to levels of 18S rRNA. Mean ± SEM, **P*<0.05 vs. control group.

Cardiac fibroblasts and cardiac myocytes were stimulated with 0.001 µg/ml, 0.01µg/ml and 0.1 µg/ml of LPS for 3 hours, and the mRNA levels were investigated using real-time qPCR (Fig. 5.2). GAPDH mRNA levels were used as the housekeeping gene.

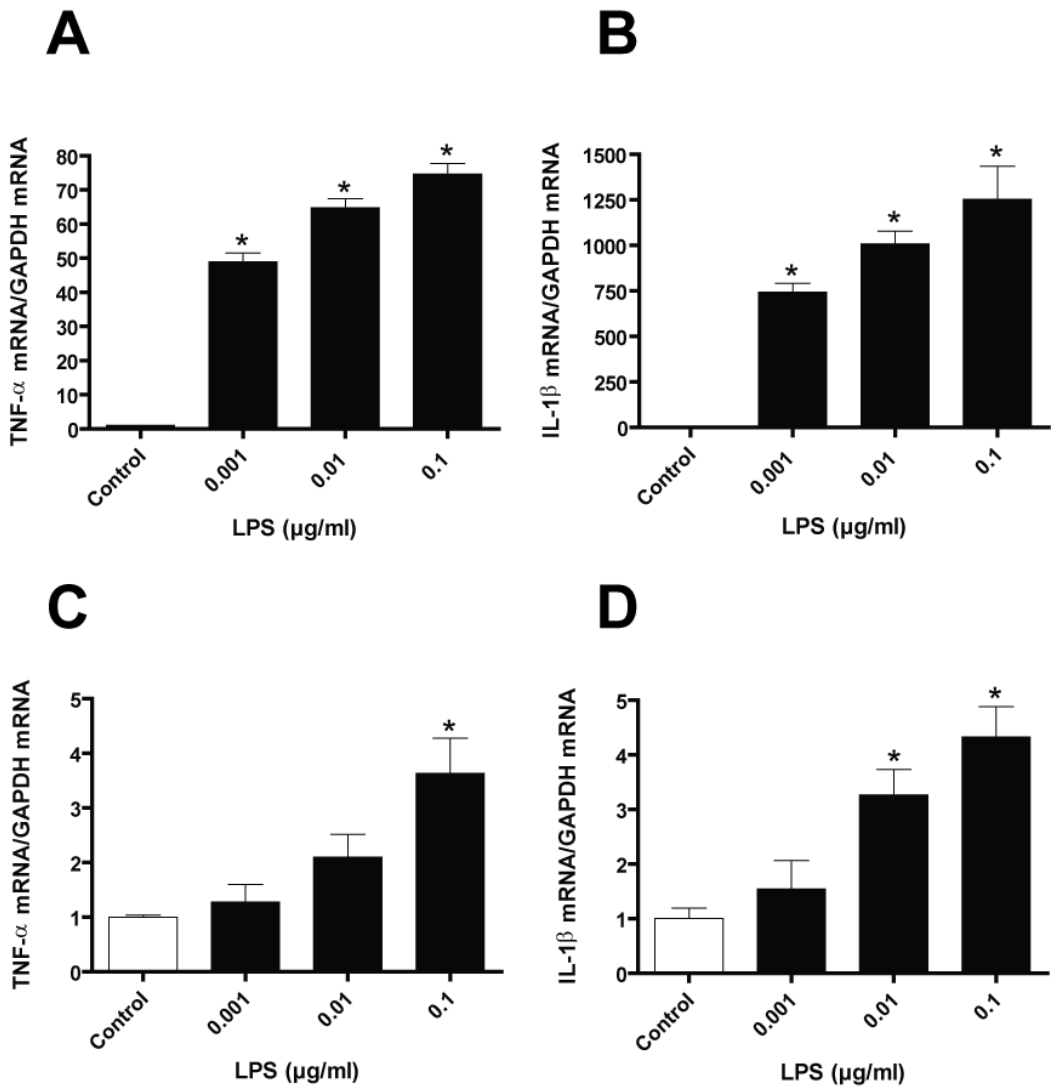

Figure 5.2 Real-time qPCR analysis demonstrating dose-dependent effects of LPS (0.001 µg/ml, 0.01 µg/ml and 0.1 µg/ml; 3hours) on mRNA levels of TNF-α and IL-1β in adult mouse cardiac fibroblasts (**A and B**) and myocytes (**C and D**), respectively. Data are presented as ratios of TNF-α or IL-1β mRNA levels relative to levels of GAPDH mRNA. Mean ± SEM, **P*<0.05 vs. control group.

Both cardiac fibroblasts and cardiac myocytes consistently responded to increasing concentrations of LPS. In cardiac fibroblasts, dramatic concentration dependent increases of TNF-α and IL-1β mRNA levels were observed in response to LPS. As shown in Fig. 5.2A, 48

fold, 64 fold and 74 fold elevations of TNF-α mRNA levels were seen in response to 0.001 µg/ml, 0.01 µg/ml and 0.1 µg/ml of LPS, respectively (P<0.001). The induction of IL-1β mRNA levels in cardiac fibroblasts in response to LPS was even more dramatic ranging from 742 fold to 1253 fold elevation of IL-1β mRNA levels in response to the lowest and highest concentrations of LPS, respectively (P<0.001), compared to non-stimulated cells (Fig. 5.2B). Adult cardiac myocytes also responded with increasing levels of TNF-α and IL-1β mRNA levels in the presence of increasing concentrations of LPS. However, fold induction of TNF-α and IL-1β in response to LPS was modest compared with that in cardiac fibroblasts. In cardiac myocytes, only 0.1 µg/ml of LPS resulted in statistically significant elevation of TNF-α mRNA levels, whereas both 0.01 µg/ml and 0.1 µg/ml of LPS resulted in statistically significant elevation of IL-1β mRNA levels. For example, stimulation of cardiac myocytes for 3 hours with 0.1 µg/ml LPS increased 3.6 fold and 4.3 fold elevations of TNF-α and IL-1β mRNA levels, respectively (P<0.05) (Fig. 5.2C and 5.2D)

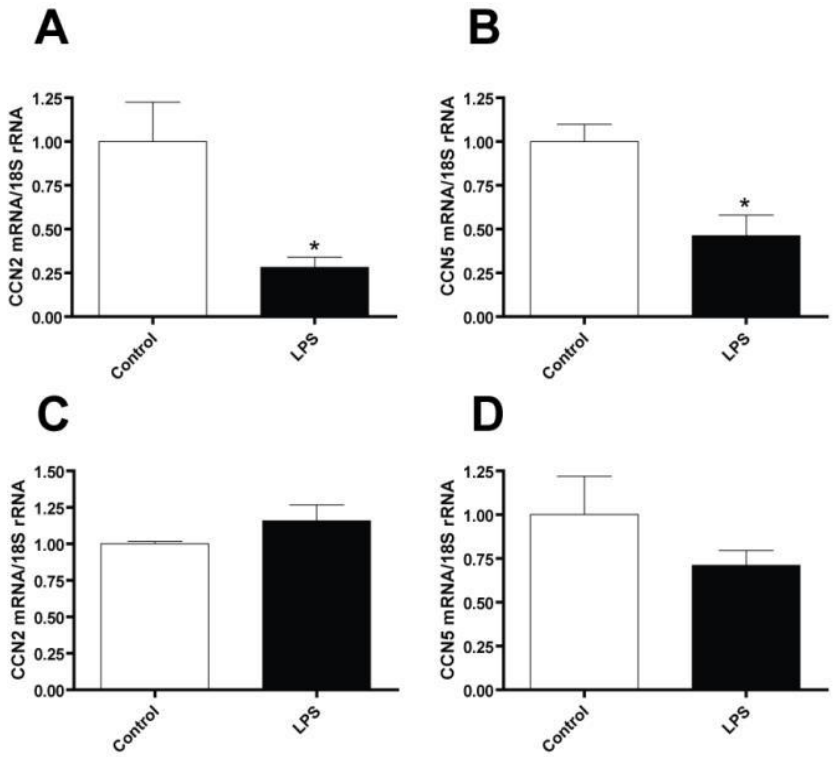

Figure 5.3 Real-time qPCR analysis depicting mRNA levels of CCN2 and CCN5 in adult mouse cardiac fibroblasts (**A and B**) and cardiac myocytes (**C and D**) stimulated with LPS (1 µg/ml: 3hours). Data are presented as ratios of CCN2 or CCN5 mRNA levels relative to levels of 18S rRNA. Mean ± SEM, *P<0.05 vs. control group.

5.2 Expression of CCN2, CCN5 and GDF15 mRNA in LPS Stimulated Cardiac Fibroblasts and Cardiac Myocytes

Recent studies have demonstrated that the matri-cellular proteins CCN2 and CCN5 and the secreted macrophage inhibitory cytokine GDF15 play cardioprotective roles under ischemia and reperfusion or chronic pressure over load induced heart failure. To investigate how the mRNA levels of CCN2, CCN5 and GDF15 in cardiac fibroblasts and cardiac myocytes respond to increasing concentrations of LPS, the mRNA levels were assayed by real-time qPCR. First, cardiac fibroblasts and cardiac myocytes were stimulated with a single concentration of LPS (1 µg/ml) and the mRNA levels of CCN2 and CCN5 were assessed by real-time qPCR. As shown in Fig. 5.3A, the mRNA levels of CCN2 were significantly down-regulated (3.5 fold; $P<0.05$) in response to LPS (1 µg/ml) in cardiac fibroblasts compared to control cells. In cardiac myocytes, no significant regulation of CCN2 mRNA expression was observed in LPS treated cells (Fig 5.3C). Similarly, the mRNA levels of CCN5 were found to be significantly down-regulated (2.2 fold; $P<0.05$) in LPS stimulated cardiac fibroblasts (Fig 5.3C) whereas in cardiac myocytes the down-regulation of CCN5 mRNA expression did not reach to the significant level in LPS treated cells compared to non-treated cells (Fig. 5.3D).

To investigate the concentration dependent effects of LPS on gene expression of these three target proteins, the primary cardiac cells were treated with three different concentrations of LPS (0.001 µg/ml, 0.01 µg/ml and 0.1 µg/ml). In cardiac fibroblasts, the mRNA levels of CCN2 were down-regulated in response to all three concentrations of LPS though statistically significant down-regulation was found only in the cells with the lowest dose of LPS stimulation (1.4 fold $P<0.05$) (Fig. 5.4A). In cardiac myocytes, the mRNA levels of CCN2 were induced in response to all three increasing concentrations of LPS though no significant induction was seen in the stimulated cells compared to the control cells (Fig. 5.4D). The mRNA levels of CCN5 were although not robustly but significantly and consistently down-regulated in cardiac fibroblasts in response to all three increasing concentrations of LPS (Fig. 5.4B). Exposure of LPS (0.001 µg/ml, 0.01 µg/ml and 0.1 µg/ml) resulted in 1.3 fold ($P<0.05$), 1.4 fold ($P<0.05$) and 1.4 fold ($P<0.001$) decreases of CCN5 mRNA levels respectively compared to the control cells. On the contrary, the mRNA levels of CCN5 tend to increase in LPS stimulated cardiac myocytes compared to control cells though the inductions were not statistically significant (Fig. 5.4E). In addition, we also investigated

GDF15 mRNA expression in response to three increasing concentrations of LPS both in cardiac fibroblasts and cardiac myocytes. The mRNA levels of GDF15 were down-regulated 1.7 fold ($P<0.05$) in cardiac fibroblasts treated cells with the lowest concentration of LPS (0.001 µg/ml), whereas down-regulation of GDF15 mRNA expressions did not reach to the significant level in cells stimulated with 0.01 µg/ml and 0.1 µg/ml of LPS compared to control cells (Fig. 5.4C). However, in cardiac myocytes, GDF15 mRNA levels were elevated in cell cultures exposed to 0.01 µg/ml (4.1 fold; $p<0.05$) and 0.1 µg/ml (6 fold; $P<0.05$) of LPS compared to control cells (Fig. 5.4F).

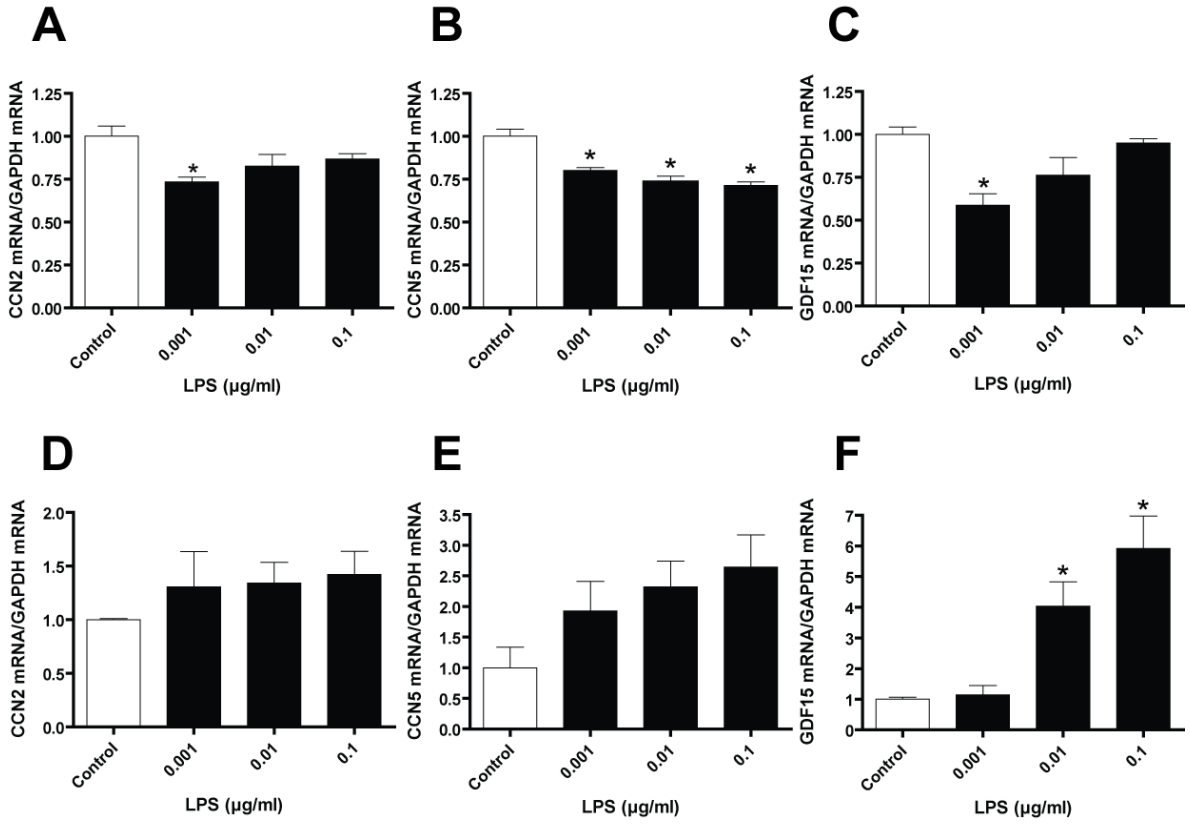

Figure 5.4 Real-time qPCR analysis depicting mRNA levels of CCN2, CCN5 and GDF15 in adult mouse cardiac fibroblasts (**A, B and C**) and cardiac myocytes (**D, E and F**) treated with increasing concentrations of LPS (0.001 µg/ml, 0.01 µg/ml and 0.1 µg/ml) for 3 hours. Data are presented as ratios of CCN2, CCN5 or GDF15 mRNA levels relative to levels of GAPDH mRNA. Mean ± SEM, *$P<0.05$ vs. control group.

5.3 Protein Expression of TNF-α and IL-1β

To assess the protein contents of the two pro-inflammatory cytokines TNF-α and IL-1β in adult cardiac fibroblasts and cardiac myocytes exposed to LPS, the cells were treated in the absence or presence of LPS (1 µg/ml) for 3 hours. Western blot analysis of extracts of cardiac fibroblasts revealed that the protein levels of TNF-α (Fig 4.5A) and IL-1β (4.5B) were

induced 2.9 fold (P<0.01) and 3.78 fold (P<0.005) respectively in LPS stimulated cells compared to control cells. On the contrary, in cardiac myocytes TNF-α and IL-1β contents remained unchanged in LPS-treated cells compared to control cells (Fig. 5.5).

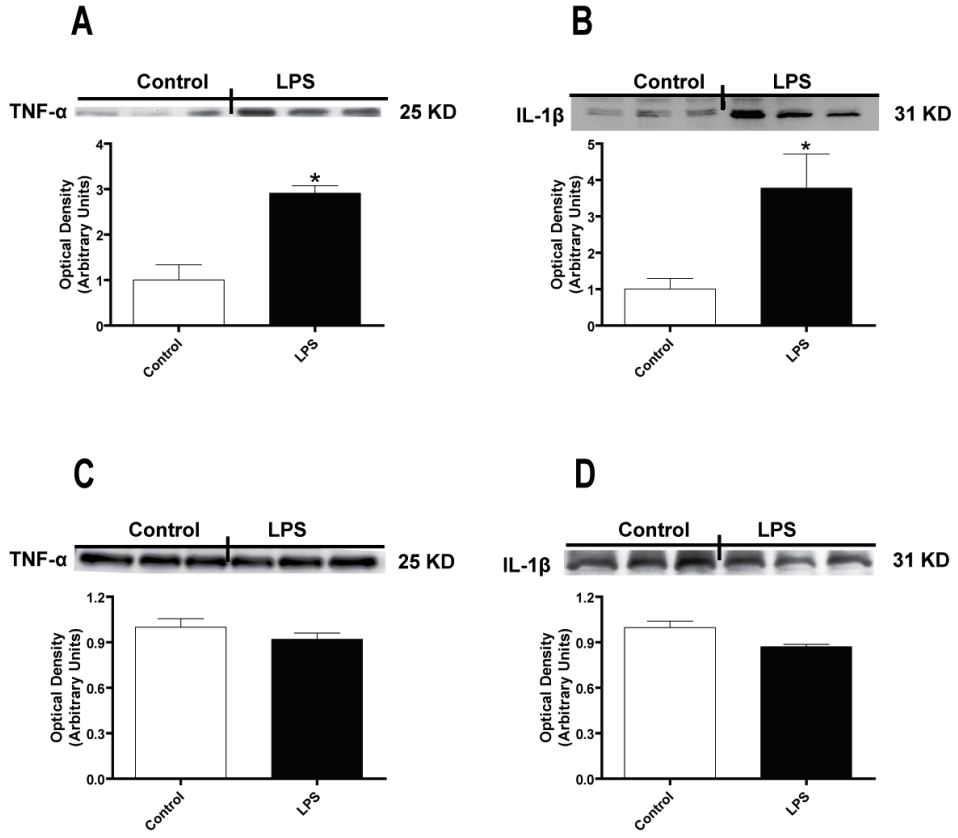

Figure 5.5 Western Blot analysis of TNF-α and IL-1β levels in adult mouse cardiac fibroblasts (**A and B**) and cardiac myocytes (**C and D**) incubated in the absence or presence of LPS (1 µg/ml) for 3 hours. Histograms demonstrate densitometric analysis of the corresponding immunoreactive bands (precursor TNF-α; 25 KD and precursor IL-1β; 31 KD). Mean ± SEM, *P<0.05 vs. control group.

5.4 Protein Expression of CCN2, CCN5 and GDF15

In order to assess CCN2, CCN5 and GDF15 contents in cardiac fibroblasts exposed to LPS, cardiac fibroblasts were stimulated with LPS (1 µg/ml) for 3 hours, 6 hours and 24 hours. Western Blot analysis of protein lysates of cardiac fibroblasts demonstrated that the CCN2 protein contents were down-regulated in LPS-treated cells compared to control cells in a time-dependent manner (3 hours, 82% of control cells, P<0.05; 6 hours, 90% of control cells, P>0.05; 24 hours, 52% of control cells, P<0.05). However, no significant regulation of CCN2 protein expression was seen in stimulated cardiac myocytes compared to control cells after 6 hour LPS stimulation (P>0.05; Fig. 5.6D). Assessment of protein contents of CCN5 and

GDF15 was also attempted, but Western blot analysis of extracts from control and LPS stimulated cardiac myocytes did not distinct immunoreactive bands.

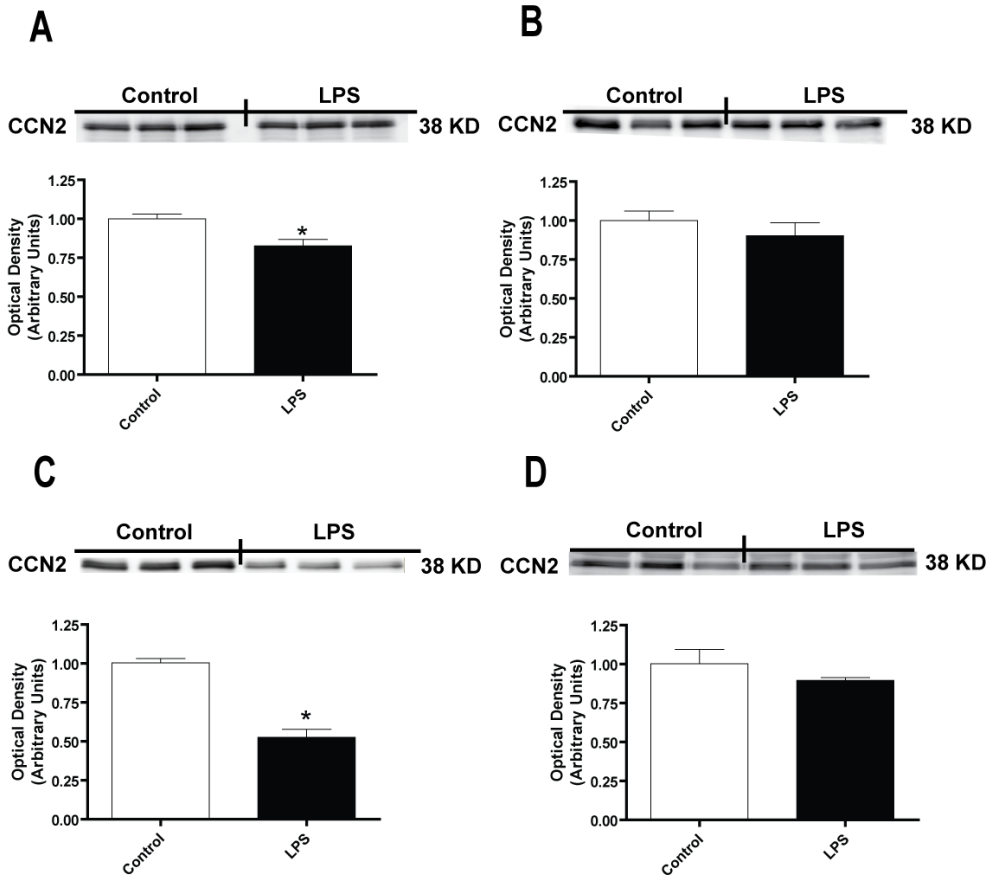

Figure 5.6 Western Blot analysis of CCN2 levels in adult mouse cardiac fibroblasts (**A-C**) and cardiac myocytes (**D**) incubated in the absence or presence of LPS (1 µg/ml). Cardiac fibroblasts were stimulated for 3(A) hours, 6(B) hours and 24(C) hours, whereas cardiac myocytes were stimulated for 6(D) hours. Histograms depict densitometric analysis of the corresponding (38 KD) immunoreactive bands. Mean ± SEM, *P<0.05 vs. control group.

5.5 Cell Viability

Assessment of LPS-induced cell death of adult cardiac myocytes was investigated by trypan blue exclusion assay. First, a time dependent experimental setup with two different concentrations of LPS (0.1 µg/ml and 10 µg/ml) was designed for the assessment of trypan blue staining of dead cardiac myocytes. Cell viability was decreased significantly and consistently after LPS treatment (Fig. 5.7A). Indeed, exposure to 0.1 µg/ml and 10 µg/ml of LPS appeared to induce similar extents of cell death (Fig. 5.7A). After 6 hours, 12 hours and 24 hours viability of cardiac myocytes exposed to 0.1 µg/ml LPS was 60.5%(P<0.05; Control cell viability 71.5%), 42% **(**P<0.001; Control cell viability 68.5%) and 43.5% (P<0.001);

Control cell viability 61%) respectively, whereas viability of cardiac myocytes exposed to 10 µg/ml LPS was 61.5% (P<0.05; Control cell viability 71.5%), 46% (P<0.001; Control cell viability 68.5%) and 34.5% (P<0.001; Control cell viability 61%) at 6 hours, 12 hours and 24 hours, respectively. In the second experiment, the old myocyte plating medium was replaced with fresh myocyte plating medium prior to start the experiment. Cell viability was assessed at 0 hours, 12 hours and 24 hours after LPS treatment (0.1 µg/ml). As shown in Fig. 5.7B cell viability was decreased in the LPS treated cells both at 12 hours (56% treated cell viability vs 78.96% control cell viability; P<0.01) and 24 hours (65.67% treated cell viability vs 79.67% control cell viability; P>0.05) though the decrease of cell viability after 24 hour LPS treatment cells did not reach to the significant level compared to control cells.

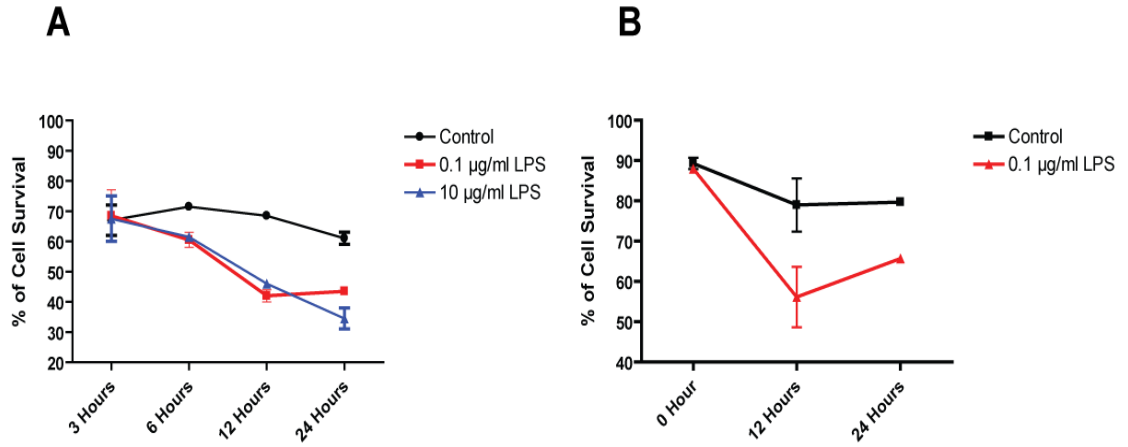

Figure 5.7 Trypan blue exclusion assay of cell viability in adult mouse cardiac myocytes after LPS stimulation. Figure **A** and **B** represent the percentage of cell survival in LPS treated cell cultures and their corresponding control cell cultures at the indicated time points. Data are presented as a percentage of living cells. P<0.05 vs. control group (Mean ± SEM) denotes statistically significant variation.

6. DISCUSSION

Mammals including humans inevitably come into contact with gram-negative bacteria and bacterial wall-associated LPS. Low-dose LPS is thought to play a positive role for the host by sensitizing the immune response and eventually enhancing resistance to infections and malignancies. However, the presence of a large amount of LPS exerts deleterious effects i.e., dramatic pathophysiological reactions e.g., fever, leukopenia, tachycardia, hypotension and multi-organ failure etc. [126]. Humans show an exquisite sensitivity to LPS with lethal range as low as 1 µg to 2 µg [127]. Lang and his colleagues injected rats with doses of endotoxin ranging from 0.01 µg/100 g body weight to 1000 µg/100 g body weight and reported that doses of 10 µg/100 g body weight or fewer were consistently nonlethal over 72 hours [128]. They also reported that doses of 100 µg/100 g body weight and 1000 µg/100 g body weight resulted in approximately 10% and 50% lethality in rats respectively after 24 hours. McDonough and his colleagues investigated myocardial performance in rodents exposed to lethal (1000 µg/100 g body weight and 100 µg/100 g body weight) and nonlethal (10 µg/100 g body weight and 1 µg/100 g body weight) doses of LPS by examining cardiac function *ex-vivo,* as used by Lang et al. [128]. They reported that the administration of endotoxin resulted in a loss of myocardial physiological reserve and this loss of myocardial reserve increased with increasing doses of endotoxin. Cardiac output was extremely sensitive to the toxic effects of endotoxin especially at elevated preload and afterload conditions. Coronary flow was decreased and thus coronary vascular resistance was elevated [129]. Shiying Tao and Thomas McKenna demonstrated that LPS (0.001-0.1µg/ml for 6 hours incubation) resulted in direct negative effects on adult rat cardiac myocyte contractile function i.e., diminished contractility by inducing NO synthase activity [130]. Rat hearts perfused with LPS (4 µg/ml) for 30 minutes showed depressed function as revealed by decreased left ventricular developed pressure and reduced peak rate of contraction and relaxation [131]. Adult mouse cardiomyocyte exposure to LPS (sub-lethal dose, 1 µg /ml for 4 to 6 hours incubation) leads to contractile dysfunction and intracellular Ca^{2+} mishandling by inducing reactive oxygen species (ROS) accumulation, protein damage and apoptosis [132]. However, inflammatory responses of adult mouse cardiac fibroblasts and cardiac myocytes to increasing concentrations of LPS are yet poorly understood.

According to prevailing studies, LPS upregulates the pro-inflammatory cytokines TNF-α and IL-1β via activation of cell signalling cascades leading to the NF-κB pathway activation

[133]. TNF-α and IL-1β both depress human myocardial function in a dose-dependent fashion [134]. In this present study, we investigated the mRNA expression of TNF-α and IL-1β in the primary adult mouse cardiac fibroblasts and cardiac myocytes in dose-dependent fashion after 3 hour LPS treatment. The finding was consistent with previous studies. LPS induced mRNA levels of TNF-α and IL-1β both in cardiac fibroblasts and cardiac myocytes in the dose-dependent manner. Both the absolute induction levels of mRNA and the relative expression levels normalized to housekeeping gene (18s rRNA or GAPDH mRNA) of these two cytokines in LPS treated cardiac fibroblasts were much higher than that in cardiac myocytes. In the normal heart, non-muscle cells comprise two-thirds of the cell population of which the majority are cardiac fibroblasts [135]. A growing body of evidence infers that cardiac fibroblasts play a pivotal role in inflammation, tissue repair, fibrosis and organogenesis by producing growth factors, cytokines, ECM proteins and proteases [136]. Protein expression levels of these cytokines were also highly induced in cardiac fibroblasts though it was only investigated by treating the cells with single concentration of LPS (1 μg/ml). Western blot analysis revealed immunoreactive bands of both cytokines corresponding to pre-cursor forms (pre-cursor TNF-α 25 KD; pre-cursor IL-1β 31 KD), but the bands corresponding to mature forms (mature TNF-α 17KD; mature IL-1β 15 KD) of cytokines were not observed. However, no significant regulation of these two cytokines at protein levels was found in cardiac myocytes after LPS treatment. The difference of induction levels of mRNA of these two cytokines between cardiac fibroblasts and cardiac myocytes might indicate a molecular mechanism of active secretion from cardiac fibroblasts at precursor level but not from cardiac myocytes. Yokoyama and his colleagues demonstrated that TNF protein synthesis in cardiac fibroblasts was 20 to 40 fold higher than that in cardiac myocytes [137]. They also showed that ANG II increased the mRNA expression and the production of biologically active TNF much higher in cardiac fibroblasts rather than in cardiac myocytes because of higher density of AT1 receptors in cardiac fibroblasts. Michio Miyoshi and colleagues demonstrated that ANG II promotes LPS-induced production of pro-inflammatory cytokines in dehydrated rats [138]. In addition,Yuanyuan Ji and his colleagues reported that ANG II contributes to TLR4 activation in vascular smooth muscle cells through AT_1 receptors and extracellular signal-regulated kinase 1/2 (ERK1/2) [139]. It is tempting to speculate that ANG II and AT_1 receptors are also involved in induction of TLR4 mRNA levels in cardiac fibroblasts since these cells, as opposed to adult cardiac myocytes, express abundant AT_1 receptors, proposing a mechanism for the robust pro-inflammatory actions of LPS in cardiac fibroblasts.

The expression of cardioprotective genes (CCN2, CCN5 and GDF15) were also investigated at mRNA and protein levels in LPS treated cardiac fibroblasts and cardiac myocytes. We found that LPS down-regulated the expression of CCN2 both at mRNA levels and protein levels in cardiac fibroblasts. The regulation of CCN expression is complex and cell specific in response to inflammation [140]. Several studies reported that TNF-α is involved in the regulation of CCN2 expression mechanisms. TNF-α induces CCN2 expression in synovial cells, whereas it inhibits CCN2 expression in chondrocytes [141, 142]. David Abraham et al., demonstrated that TNF-α inhibits TGF-β induced CCN2 expression in normal cultured fibroblasts via cis-elements located between -244 and -166 of the CCN2 promoter [143]. Fun Yu et al., also showed that TNF-α inhibits TGF-β induced CCN2 expression in embryonic fibroblasts by swapping the binding preference of p300 from Smad4 to p65 [144]. This finding infers that p300 physically binds with p65 rather than Smad4 in the presence of both TNF-alpha and TGF-beta and eventually results in inhibition of CCN2 expression. We also found that the mRNA expression of CCN5 was down-regulated after LPS treatment though CCN5 expression at protein level was not detected by Western blot analysis. Either the primary antibody used in Western blot analysis does not have the specificity for murine endogenous CCN5 protein or the cellular CCN5 protein levels were too low to detect. No previous study has demonstrated down-regulation of CCN5 in response to LPS in cardiac fibroblasts. To be speculative, it is tempting to deduce that the down regulation of CCN5 by LPS is conferred by the same mechanism that has been described for CCN2, since CCN5 belongs to CCN family of the genes. Laure Rittié and his colleagues demonstrated that both CCN2 and CCN5 mRNA expression levels were strongly down-regulated during wound healing in response to skin inflammation [145]. The present study revealed that the mRNA expression of GDF15 was significantly down-regulated in adult mouse cardiac fibroblasts after 0.001 µg/ml of LPS treatment for 3 hours. However, the role of cardiac GDF15 during sepsis is not well elucidated by previous studies. It might be anticipated that either LPS or cytokines may interfere the transcription level of GDF15 in cardiac fibroblasts to inhibit the mRNA expression. Again, we could not detect GDF15 expression at protein levels in cardiac fibroblasts. Either the primary antibody used had not cross-reactivity with murine cells or the cellular GDF15 protein levels were too low to detect.

On the other hand in cardiac myocytes, CCN2 and CCN5 mRNA levels tended to increase after stimulation with increasing concentrations of LPS although not statistically significant.

However, no regulation of CCN2 expression was detected at protein levels in LPS treated cardiac myocytes, whereas CCN5 protein expression remained undetectable in cardiac myocytes. Our data showed significant up-regulation of GDF15 at mRNA expression levels in cardiac myocytes after treatment with increasing concentrations of LPS. Previous studies reported that GDF15 expression was rapidly induced by the pro-inflammatory cytokines TNF-α and IL-1β which results in modulation of macrophage activation and inflammation [146]. However, it is yet unknown how the inflammatory cytokines induce GDF15 expression. Although, GDF15 mRNA was significantly upregulated in LPS-treated cardiac myocytes, we were not able to detect GDF15 expression at protein levels after LPS treatment.

We investigated cell death by trypan blue exclusion assay in isolated adult mouse cardiac myocytes. LPS (0.1 and 10 µg/ml) significantly decreased cell viability in a time dependent manner. In our first experiment LPS-treated cells displayed significantly decreased viability after 6 hours, 12 hours and 24 hours. The experiment was repeated with minor modification by replacing the old myocyte plating medium with fresh myocyte plating medium to avoid the background levels of enzymes released before start of the experiment. In the latter experiment, LPS significantly decreased cell viability after 12 hours though it showed no significant reduction in cell viability after 24 hours. The possible reason for not getting significant cell death at the 24 hour time point might be that 24 hours of incubation of cells resulted in many dead cells detaching from the surface of the well which might have been excluded during counting period and eventually might have given a non-significant reduction. Cardiac myocytes have limited ability to regenerate and in heart failure apoptosis results in continuous loss of cardiac myocytes [147]. Several studies reported that LPS induces cardiac apoptosis in sepsis [148, 149]. Li et al. reported that a single dose of LPS that results in no stress and does not impact on blood pressure is sufficient enough to induce cardiac apoptosis via AT_1 receptors [150]. Frantz and his colleagues reported that the abundant expression of the LPS receptor, TLR4 on cardiomyocytes makes the heart sensitive to LPS [151]. LPS-induced apoptosis in cardiomyocytes has been shown to be TNF-α dependent via the CD14 signaling pathway [152]. Sandra demonstrated that TNF-α signaling provokes apoptosis of cardiomyocytes through activation of multiple cell death pathways [153]. A putative mechanism is that LPS-induced release of TNF-α from cardiac fibroblasts exerts direct cytotoxic effects on neighboring cardiac myocytes since release of TNF-α is more robust from cardiac fibroblasts than from cardiac myocytes.

7. CONCLUSION

In conclusion, LPS plays a pivotal role in cardiac dysfunction and remodelling by inducing a release of inflammatory cytokines in the heart. Our *in vitro* data demonstrated that LPS induces the production of the pro-inflammatory cytokines TNF-α and IL-1β in adult mouse cardiac fibroblasts and myocytes suggesting a huge release of TNF-α and IL-1β particularly from cardiac fibroblasts. We also reported that LPS downregulates CCN2 and CCN5 expression in cardiac fibroblasts and induces GDF15 expression in cardiac myocytes. We found that LPS decreases cardiac myocyte viability in a time dependent manner. In our future studies, we will investigate the cytoprotective effects of recombinant CCN2, CCN5 and GDF15 at LPS-induced cell death in cardiac cell cultures. Our group already developed transgenic mice with cardiac-restricted over-expression of CCN2. It would also be interesting to delineate the effects of LPS *in vivo* using the CCN2-transgenic mouse model.

8. REFERENCES

1. Bone, R.C., et al., *Definitions for sepsis and organ failure and guidelines for the use of innovative therapies in sepsis. The ACCP/SCCM Consensus Conference Committee. American College of Chest Physicians/Society of Critical Care Medicine.* Chest, 1992. **101**(6): p. 1644-55.
2. Warren, H.S., *Strategies for the treatment of sepsis.* N Engl J Med, 1997. **336**(13): p. 952-3.
3. Stone, R., *Search for sepsis drugs goes on despite past failures.* Science, 1994. **264**(5157): p. 365-7.
4. Angus, D.C., et al., *Epidemiology of severe sepsis in the United States: analysis of incidence, outcome, and associated costs of care.* Crit Care Med, 2001. **29**(7): p. 1303-10.
5. Dombrovskiy, V.Y., et al., *Rapid increase in hospitalization and mortality rates for severe sepsis in the United States: a trend analysis from 1993 to 2003.* Crit Care Med, 2007. **35**(5): p. 1244-50.
6. Annane, D., E. Bellissant, and J.M. Cavaillon, *Septic shock.* Lancet, 2005. **365**(9453): p. 63-78.
7. Robertson, C.M. and C.M. Coopersmith, *The systemic inflammatory response syndrome.* Microbes Infect, 2006. **8**(5): p. 1382-9.
8. Waisbren, B.A., *Bacteremia due to gram-negative bacilli other than the Salmonella; a clinical and therapeutic study.* AMA Arch Intern Med, 1951. **88**(4): p. 467-88.
9. Levy, M.M., et al., *2001 SCCM/ESICM/ACCP/ATS/SIS International Sepsis Definitions Conference.* Crit Care Med, 2003. **31**(4): p. 1250-6.
10. Parker, M.M., et al., *Profound but reversible myocardial depression in patients with septic shock.* Ann Intern Med, 1984. **100**(4): p. 483-90.
11. Ognibene, F.P., et al., *Depressed left ventricular performance. Response to volume infusion in patients with sepsis and septic shock.* Chest, 1988. **93**(5): p. 903-10.
12. Parker, M.M., et al., *Right ventricular dysfunction and dilatation, similar to left ventricular changes, characterize the cardiac depression of septic shock in humans.* Chest, 1990. **97**(1): p. 126-31.
13. Jardin, F., et al., *Persistent preload defect in severe sepsis despite fluid loading: A longitudinal echocardiographic study in patients with septic shock.* Chest, 1999. **116**(5): p. 1354-9.

14. Vieillard-Baron, A., et al., *Actual incidence of global left ventricular hypokinesia in adult septic shock.* Crit Care Med, 2008. **36**(6): p. 1701-6.
15. Bouhemad, B., et al., *Acute left ventricular dilatation and shock-induced myocardial dysfunction.* Crit Care Med, 2009. **37**(2): p. 441-7.
16. Cunnion, R.E., et al., *The coronary circulation in human septic shock.* Circulation, 1986. **73**(4): p. 637-44.
17. Hinshaw, L.B., *Sepsis/septic shock: participation of the microcirculation: an abbreviated review.* Crit Care Med, 1996. **24**(6): p. 1072-8.
18. Groeneveld, A.B., et al., *Maldistribution of heterogeneous coronary blood flow during canine endotoxin shock.* Cardiovasc Res, 1991. **25**(1): p. 80-8.
19. R. S. Hotchkiss, S.K.S., J. J. Neil, R. D. Chen, J. K. Manchester, I. E. Karl, O. H. Lowry, and J. J. Ackerman, *Sepsis does not impair tricarboxylic acid cycle in the heart.* American Journal of Physiology - Cell Physiology 1991.
20. Lefer, A.M., *Role of a myocardial depressant factor in the pathogenesis of circulatory shock.* Fed Proc, 1970. **29**(6): p. 1836-47.
21. Lefer, A.M. and M.J. Rovetto, *Influence of a myocardial depressant factor on physiologic properties of cardiac muscle.* Proc Soc Exp Biol Med, 1970. **134**(1): p. 269-73.
22. Parrillo, J.E., et al., *A circulating myocardial depressant substance in humans with septic shock. Septic shock patients with a reduced ejection fraction have a circulating factor that depresses in vitro myocardial cell performance.* J Clin Invest, 1985. **76**(4): p. 1539-53.
23. Hoffmann, J.N., et al., *Hemofiltrate from patients with severe sepsis and depressed left ventricular contractility contains cardiotoxic compounds.* Shock, 1999. **12**(3): p. 174-80.
24. Suffredini, A.F., et al., *The cardiovascular response of normal humans to the administration of endotoxin.* N Engl J Med, 1989. **321**(5): p. 280-7.
25. Tavener, S.A. and P. Kubes, *Is there a role for cardiomyocyte toll-like receptor 4 in endotoxemia?* Trends Cardiovasc Med, 2005. **15**(5): p. 153-7.
26. Tavener, S.A., et al., *Immune cell Toll-like receptor 4 is required for cardiac myocyte impairment during endotoxemia.* Circ Res, 2004. **95**(7): p. 700-7.
27. Hunter, J.D. and M. Doddi, *Sepsis and the heart.* Br J Anaesth. **104**(1): p. 3-11.
28. Massion, P.B., et al., *Nitric oxide and cardiac function: ten years after, and continuing.* Circ Res, 2003. **93**(5): p. 388-98.

29. Massion, P.B., S. Moniotte, and J.L. Balligand, *Nitric oxide: does it play a role in the heart of the critically ill?* Curr Opin Crit Care, 2001. **7**(5): p. 323-36.
30. Vallance, P. and S. Moncada, *Role of endogenous nitric oxide in septic shock.* New Horiz, 1993. **1**(1): p. 77-86.
31. Brady, A.J. and P.A. Poole-Wilson, *Circulatory failure in septic shock. Nitric oxide: too much of a good thing?* Br Heart J, 1993. **70**(2): p. 103-5.
32. Kelm M, S.S., Dahmann R, Dolu B, Perings S, Decking UK, Schrader J, Strauer BE, *Nitric oxide induced contractile dysfunction is related to a reduction in myocardial energy generation.* Cardiovascular Research, 1997. **36**: p. 185-94.
33. Kawaguchi, H., et al., *In vivo gene transfection of human endothelial cell nitric oxide synthase in cardiomyocytes causes apoptosis-like cell death. Identification using Sendai virus-coated liposomes.* Circulation, 1997. **95**(10): p. 2441-7.
34. Rudiger, A. and M. Singer, *Mechanisms of sepsis-induced cardiac dysfunction.* Crit Care Med, 2007. **35**(6): p. 1599-608.
35. Latour, B., *Pasteur - Une Science, Un Style, Un Siècle.* Libraire Académique, 1994.
36. Brieger, A.L., *Ueber Ptomaine* Hirschwald, 1886.
37. Koch, R., *R. Koch's Vortrag über die Cholera.* Fortschr Med, 1884.
38. Pfeiffer, R., 1–16 (). *Weitere Untersuchungen über das Wesen der Choleraimmunität und über spezifisch bacterizide Prozesse.* Z. Hyg, 1894.
39. Pfeiffer, R., *Untersuchungen über das Choleragift.* Z. Hyg, 1892.
40. Wolff, A., *Über Grundgesetze der Immunität* Zentralbl Bakteriol, 1904.
41. Centanni, E., *Untersuchungen über das Infektionsfieber -das Fiebergift der Bakterien.* Dtsch. Med. Wochenschr, 1894.
42. Nauts, H.C., W.E. Swift, and B.L. Coley, *The treatment of malignant tumors by bacterial toxins as developed by the late William B. Coley, M.D., reviewed in the light of modern research.* Cancer Res, 1946. **6**: p. 205-16.
43. Beutler, B. and E.T. Rietschel, *Innate immune sensing and its roots: the story of endotoxin.* Nat Rev Immunol, 2003. **3**(2): p. 169-76.
44. Rietschel, E.T.W., O., *Endotoxin in Health and Disease.* Marcel Dekker, New York, 1999.
45. Shear, M.J.T., F. C. , *Chemical treatment of tumors. V. Isolation of the hemorrhage-producing fraction rom Serratia marcescens (Bacillus prodigiosus) culture filtrates.* J. Natl Cancer Inst., 1943.
46. Raetz, C.R., *Biochemistry of endotoxins.* Annu Rev Biochem, 1990. **59**: p. 129-70.

47. Raetz, C.R. and C. Whitfield, *Lipopolysaccharide endotoxins.* Annu Rev Biochem, 2002. **71**: p. 635-700.
48. Galanos, C., et al., *Synthetic and natural Escherichia coli free lipid A express identical endotoxic activities.* Eur J Biochem, 1985. **148**(1): p. 1-5.
49. Schromm, A.B., et al., *The charge of endotoxin molecules influences their conformation and IL-6-inducing capacity.* J Immunol, 1998. **161**(10): p. 5464-71.
50. Wright, S.D., et al., *CD14, a receptor for complexes of lipopolysaccharide (LPS) and LPS binding protein.* Science, 1990. **249**(4975): p. 1431-3.
51. Lu, Y.C., W.C. Yeh, and P.S. Ohashi, *LPS/TLR4 signal transduction pathway.* Cytokine, 2008. **42**(2): p. 145-51.
52. Poltorak, A., et al., *Defective LPS signaling in C3H/HeJ and C57BL/10ScCr mice: mutations in Tlr4 gene.* Science, 1998. **282**(5396): p. 2085-8.
53. Gioannini, T.L. and J.P. Weiss, *Regulation of interactions of Gram-negative bacterial endotoxins with mammalian cells.* Immunol Res, 2007. **39**(1-3): p. 249-60.
54. Tobias, P.S., K. Soldau, and R.J. Ulevitch, *Isolation of a lipopolysaccharide-binding acute phase reactant from rabbit serum.* J Exp Med, 1986. **164**(3): p. 777-93.
55. Wright, S.D., et al., *Lipopolysaccharide (LPS) binding protein opsonizes LPS-bearing particles for recognition by a novel receptor on macrophages.* J Exp Med, 1989. **170**(4): p. 1231-41.
56. Miyake, K., *Innate immune sensing of pathogens and danger signals by cell surface Toll-like receptors.* Semin Immunol, 2007. **19**(1): p. 3-10.
57. Shimazu, R., et al., *MD-2, a molecule that confers lipopolysaccharide responsiveness on Toll-like receptor 4.* J Exp Med, 1999. **189**(11): p. 1777-82.
58. Nagai, Y., et al., *Essential role of MD-2 in LPS responsiveness and TLR4 distribution.* Nat Immunol, 2002. **3**(7): p. 667-72.
59. Gioannini, T.L., et al., *Isolation of an endotoxin-MD-2 complex that produces Toll-like receptor 4-dependent cell activation at picomolar concentrations.* Proc Natl Acad Sci U S A, 2004. **101**(12): p. 4186-91.
60. Mitsuzawa, H., et al., *Recombinant soluble forms of extracellular TLR4 domain and MD-2 inhibit lipopolysaccharide binding on cell surface and dampen lipopolysaccharide-induced pulmonary inflammation in mice.* J Immunol, 2006. **177**(11): p. 8133-9.
61. Fitzgerald, K.A., D.C. Rowe, and D.T. Golenbock, *Endotoxin recognition and signal transduction by the TLR4/MD2-complex.* Microbes Infect, 2004. **6**(15): p. 1361-7.

62. Lord, K.A., B. Hoffman-Liebermann, and D.A. Liebermann, *Nucleotide sequence and expression of a cDNA encoding MyD88, a novel myeloid differentiation primary response gene induced by IL6.* Oncogene, 1990. **5**(7): p. 1095-7.
63. Balija, T.M. and S.F. Lowry, *Lipopolysaccharide and sepsis-associated myocardial dysfunction.* Curr Opin Infect Dis, 2011. **24**(3): p. 248-53.
64. Jianhui, L., et al., *Endotoxin impairs cardiac hemodynamics by affecting loading conditions but not by reducing cardiac inotropism.* Am J Physiol Heart Circ Physiol, 2010. **299**(2): p. H492-501.
65. Davani, E.Y., et al., *Cardiac ICAM-1 mediates leukocyte-dependent decreased ventricular contractility in endotoxemic mice.* Cardiovasc Res, 2006. **72**(1): p. 134-42.
66. Ichinose, F., et al., *Cardiomyocyte-specific overexpression of nitric oxide synthase 3 prevents myocardial dysfunction in murine models of septic shock.* Circ Res, 2007. **100**(1): p. 130-9.
67. Pinsky, M.R. and P. Rico, *Cardiac contractility is not depressed in early canine endotoxic shock.* Am J Respir Crit Care Med, 2000. **161**(4 Pt 1): p. 1087-93.
68. Kober, P.M., J.X. Thomas, Jr., and R.M. Raymond, *Increased myocardial contractility during endotoxin shock in dogs.* Am J Physiol, 1985. **249**(4 Pt 2): p. H715-22.
69. Hassoun, S.M., et al., *Prevention of endotoxin-induced sarcoplasmic reticulum calcium leak improves mitochondrial and myocardial dysfunction.* Crit Care Med, 2008. **36**(9): p. 2590-6.
70. Duncan, D.J., et al., *TNF-alpha and IL-1beta increase Ca2+ leak from the sarcoplasmic reticulum and susceptibility to arrhythmia in rat ventricular myocytes.* Cell Calcium, 2010. **47**(4): p. 378-86.
71. Kao, Y.H., et al., *Tumor necrosis factor-alpha decreases sarcoplasmic reticulum Ca2+-ATPase expressions via the promoter methylation in cardiomyocytes.* Crit Care Med, 2010. **38**(1): p. 217-22.
72. Lancel, S., et al., *Ventricular myocyte caspases are directly responsible for endotoxin-induced cardiac dysfunction.* Circulation, 2005. **111**(20): p. 2596-604.
73. Neviere, R., et al., *Caspase-dependent protein phosphatase 2A activation contributes to endotoxin-induced cardiomyocyte contractile dysfunction.* Crit Care Med, 2010. **38**(10): p. 2031-6.

74. Fallach, R., et al., *Cardiomyocyte Toll-like receptor 4 is involved in heart dysfunction following septic shock or myocardial ischemia.* J Mol Cell Cardiol, 2010. **48**(6): p. 1236-44.
75. Kleinbongard, P., R. Schulz, and G. Heusch, *TNFalpha in myocardial ischemia/reperfusion, remodeling and heart failure.* Heart Fail Rev, 2011. **16**(1): p. 49-69.
76. Carswell, E.A., et al., *An endotoxin-induced serum factor that causes necrosis of tumors.* Proc Natl Acad Sci U S A, 1975. **72**(9): p. 3666-70.
77. Aker, S., et al., *Serum but not myocardial TNF-alpha concentration is increased in pacing-induced heart failure in rabbits.* Am J Physiol Regul Integr Comp Physiol, 2003. **285**(2): p. R463-9.
78. Arras, M., et al., *Tumor necrosis factor-alpha in macrophages of heart, liver, kidney, and in the pituitary gland.* Cell Tissue Res, 1996. **285**(1): p. 39-49.
79. Frangogiannis, N.G., et al., *Resident cardiac mast cells degranulate and release preformed TNF-alpha, initiating the cytokine cascade in experimental canine myocardial ischemia/reperfusion.* Circulation, 1998. **98**(7): p. 699-710.
80. Huang, C.H., et al., *Role of the innate immune system in acute viral myocarditis.* Basic Res Cardiol, 2009. **104**(3): p. 228-37.
81. Roman-Campos, D., et al., *Changes in cellular contractility and cytokines profile during Trypanosoma cruzi infection in mice.* Basic Res Cardiol, 2009. **104**(3): p. 238-46.
82. Lula, J.F., et al., *Plasma concentrations of tumour necrosis factor-alpha, tumour necrosis factor-related apoptosis-inducing ligand, and FasLigand/CD95L in patients with Chagas cardiomyopathy correlate with left ventricular dysfunction.* Eur J Heart Fail, 2009. **11**(9): p. 825-31.
83. Ba, X., et al., *Trypanosoma cruzi induces the reactive oxygen species-PARP-1-RelA pathway for up-regulation of cytokine expression in cardiomyocytes.* J Biol Chem, 2010. **285**(15): p. 11596-606.
84. Gilles, S., et al., *Release of TNF-alpha during myocardial reperfusion depends on oxidative stress and is prevented by mast cell stabilizers.* Cardiovasc Res, 2003. **60**(3): p. 608-16.
85. Dorge, H., et al., *Coronary microembolization: the role of TNF-alpha in contractile dysfunction.* J Mol Cell Cardiol, 2002. **34**(1): p. 51-62.

86. Reil, J.C., et al., *Insights from knock-out models concerning postischemic release of TNFalpha from isolated mouse hearts.* J Mol Cell Cardiol, 2007. **42**(1): p. 133-41.
87. Skyschally, A., et al., *Bidirectional role of tumor necrosis factor-alpha in coronary microembolization: progressive contractile dysfunction versus delayed protection against infarction.* Circ Res, 2007. **100**(1): p. 140-6.
88. Skyschally, A., et al., *Coronary microembolization.* Basic Res Cardiol, 2006. **101**(5): p. 373-82.
89. Dinarello, C.A., *Biologic basis for interleukin-1 in disease.* Blood, 1996. **87**(6): p. 2095-147.
90. Dinarello, C.A., *Cytokines as endogenous pyrogens.* J Infect Dis, 1999. **179 Suppl 2**: p. S294-304.
91. Dinarello, C.A., *Interleukin-1beta.* Crit Care Med, 2005. **33**(12 Suppl): p. S460-2.
92. Dinarello, C.A., *The role of the interleukin-1-receptor antagonist in blocking inflammation mediated by interleukin-1*. N Engl J Med, 2000. **343**(10): p. 732-4.
93. Matsushima, K. and J.J. Oppenheim, *Interleukin 8 and MCAF: novel inflammatory cytokines inducible by IL 1 and TNF*. Cytokine, 1989. **1**(1): p. 2-13.
94. Marui, N., et al., *Vascular cell adhesion molecule-1 (VCAM-1) gene transcription and expression are regulated through an antioxidant-sensitive mechanism in human vascular endothelial cells.* J Clin Invest, 1993. **92**(4): p. 1866-74.
95. Bujak, M. and N.G. Frangogiannis, *The role of IL-1 in the pathogenesis of heart disease.* Arch Immunol Ther Exp (Warsz), 2009. **57**(3): p. 165-76.
96. Bork, P., *The modular architecture of a new family of growth regulators related to connective tissue growth factor*. FEBS Lett, 1993. **327**(2): p. 125-30.
97. Lau, L.F. and S.C. Lam, *The CCN family of angiogenic regulators: the integrin connection.* Exp Cell Res, 1999. **248**(1): p. 44-57.
98. Kim, H.S., et al., *Identification of a family of low-affinity insulin-like growth factor binding proteins (IGFBPs): characterization of connective tissue growth factor as a member of the IGFBP superfamily*. Proc Natl Acad Sci U S A, 1997. **94**(24): p. 12981-6.
99. Luo, Q., et al., *Connective tissue growth factor (CTGF) is regulated by Wnt and bone morphogenetic proteins signaling in osteoblast differentiation of mesenchymal stem cells.* J Biol Chem, 2004. **279**(53): p. 55958-68.

100. Bradham, D.M., et al., *Connective tissue growth factor: a cysteine-rich mitogen secreted by human vascular endothelial cells is related to the SRC-induced immediate early gene product CEF-10.* J Cell Biol, 1991. **114**(6): p. 1285-94.
101. Rachfal, A.W. and D.R. Brigstock, *Structural and functional properties of CCN proteins.* Vitam Horm, 2005. **70**: p. 69-103.
102. de Winter, P., P. Leoni, and D. Abraham, *Connective tissue growth factor: structure-function relationships of a mosaic, multifunctional protein.* Growth Factors, 2008. **26**(2): p. 80-91.
103. Daniels, A., et al., *Connective tissue growth factor and cardiac fibrosis.* Acta Physiol (Oxf), 2009. **195**(3): p. 321-38.
104. Leask, A., *Potential therapeutic targets for cardiac fibrosis: TGFbeta, angiotensin, endothelin, CCN2, and PDGF, partners in fibroblast activation.* Circ Res, 2010. **106**(11): p. 1675-80.
105. Ahmed, M.S., et al., *Mechanisms of novel cardioprotective functions of CCN2/CTGF in myocardial ischemia-reperfusion injury.* Am J Physiol Heart Circ Physiol, 2011. **300**(4): p. H1291-302.
106. Ahmed, M.S., et al., *Connective tissue growth factor--a novel mediator of angiotensin II-stimulated cardiac fibroblast activation in heart failure in rats.* J Mol Cell Cardiol, 2004. **36**(3): p. 393-404.
107. Chen, C.C. and L.F. Lau, *Functions and mechanisms of action of CCN matricellular proteins.* Int J Biochem Cell Biol, 2009. **41**(4): p. 771-83.
108. Brigstock, D.R., *The CCN family: a new stimulus package.* J Endocrinol, 2003. **178**(2): p. 169-75.
109. Ball, D.K., et al., *Characterization of 16- to 20-kilodalton (kDa) connective tissue growth factors (CTGFs) and demonstration of proteolytic activity for 38-kDa CTGF in pig uterine luminal flushings.* Biol Reprod, 1998. **59**(4): p. 828-35.
110. Kubota, S. and M. Takigawa, *CCN family proteins and angiogenesis: from embryo to adulthood.* Angiogenesis, 2007. **10**(1): p. 1-11.
111. Yoon, P.O., et al., *The opposing effects of CCN2 and CCN5 on the development of cardiac hypertrophy and fibrosis.* J Mol Cell Cardiol, 2010. **49**(2): p. 294-303.
112. Leask, A. and D.J. Abraham, *All in the CCN family: essential matricellular signaling modulators emerge from the bunker.* J Cell Sci, 2006. **119**(Pt 23): p. 4803-10.

113. Bootcov, M.R., et al., *MIC-1, a novel macrophage inhibitory cytokine, is a divergent member of the TGF-beta superfamily.* Proc Natl Acad Sci U S A, 1997. **94**(21): p. 11514-9.
114. Taddei, S. and A. Virdis, *Growth differentiation factor-15 and cardiovascular dysfunction and disease: malefactor or innocent bystander?* Eur Heart J, 2010. **31**(10): p. 1168-71.
115. Tan, M., et al., *PTGF-beta, a type beta transforming growth factor (TGF-beta) superfamily member, is a p53 target gene that inhibits tumor cell growth via TGF-beta signaling pathway.* Proc Natl Acad Sci U S A, 2000. **97**(1): p. 109-14.
116. Kempf, T., et al., *The transforming growth factor-beta superfamily member growth-differentiation factor-15 protects the heart from ischemia/reperfusion injury.* Circ Res, 2006. **98**(3): p. 351-60.
117. Xu, J., et al., *GDF15/MIC-1 functions as a protective and antihypertrophic factor released from the myocardium in association with SMAD protein activation.* Circ Res, 2006. **98**(3): p. 342-50.
118. O'Connell, T.D., M.C. Rodrigo, and P.C. Simpson, *Isolation and culture of adult mouse cardiac myocytes.* Methods Mol Biol, 2007. **357**: p. 271-96.
119. Rekosh, D.M., H. Lodish, and D. Baltimore, *Protein synthesis in Escherichia coli extracts programmed by poliovirus RNA.* J Mol Biol, 1970. **54**(2): p. 327-40.
120. Towbin, H., T. Staehelin, and J. Gordon, *Electrophoretic transfer of proteins from polyacrylamide gels to nitrocellulose sheets: procedure and some applications.* Proc Natl Acad Sci U S A, 1979. **76**(9): p. 4350-4.
121. Bassara, H. and C. Ramlau, *[Use of the preparation Orimeten in the treatment of advanced cases of breast cancer in women]*. Nowotwory, 1987. **37**(2): p. 148-53.
122. Bergendahl, V., B.T. Glaser, and R.R. Burgess, *A fast Western blot procedure improved for quantitative analysis by direct fluorescence labeling of primary antibodies.* J Immunol Methods, 2003. **277**(1-2): p. 117-25.
123. Alegria-Schaffer, A., A. Lodge, and K. Vattem, *Performing and optimizing Western blots with an emphasis on chemiluminescent detection.* Methods Enzymol, 2009. **463**: p. 573-99.
124. Mattson, D.L. and T.G. Bellehumeur, *Comparison of three chemiluminescent horseradish peroxidase substrates for immunoblotting.* Anal Biochem, 1996. **240**(2): p. 306-8.

125. Walker, G.R., Feather, K. D., Davis, P. D., and Hines, K. K., *SuperSignalTM CL-HRP: A new enhanced chemiluminescent substrate for the development of the horseradish peroxide label in Western blotting applications.* J. NIH Res, 1995. **7**(76).
126. Schletter, J., et al., *Molecular mechanisms of endotoxin activity.* Arch Microbiol, 1995. **164**(6): p. 383-9.
127. Sauter, C. and C. Wolfensberger, *Interferon in human serum after injection of endotoxin.* Lancet, 1980. **2**(8199): p. 852-3.
128. Lang, C.H., G.J. Bagby, and J.J. Spitzer, *Glucose kinetics and body temperature after lethal and nonlethal doses of endotoxin.* Am J Physiol, 1985. **248**(4 Pt 2): p. R471-8.
129. McDonough, K.H., B.A. Brumfield, and C.H. Lang, *In vitro myocardial performance after lethal and nonlethal doses of endotoxin.* Am J Physiol, 1986. **250**(2 Pt 2): p. H240-6.
130. Tao, S. and T.M. McKenna, *In vitro endotoxin exposure induces contractile dysfunction in adult rat cardiac myocytes.* Am J Physiol, 1994. **267**(5 Pt 2): p. H1745-52.
131. An, J., et al., *Differential sensitivity to LPS-induced myocardial dysfunction in the isolated brown Norway and Dahl S rat hearts: roles of mitochondrial function, NF-kappaB activation, and TNF-alpha production.* Shock, 2012. **37**(3): p. 325-32.
132. Zhao, P., et al., *Cardiac-specific overexpression of insulin-like growth factor I (IGF-1) rescues lipopolysaccharide-induced cardiac dysfunction and activation of stress signaling in murine cardiomyocytes.* Shock, 2009. **32**(1): p. 100-7.
133. Nduka, O.O. and J.E. Parrillo, *The pathophysiology of septic shock.* Crit Care Clin, 2009. **25**(4): p. 677-702, vii.
134. Cain, B.S., et al., *Tumor necrosis factor-alpha and interleukin-1beta synergistically depress human myocardial function.* Crit Care Med, 1999. **27**(7): p. 1309-18.
135. Maisch, B., *Extracellular matrix and cardiac interstitium: restriction is not a restricted phenomenon.* Herz, 1995. **20**(2): p. 75-80.
136. Manabe, I., T. Shindo, and R. Nagai, *Gene expression in fibroblasts and fibrosis: involvement in cardiac hypertrophy.* Circ Res, 2002. **91**(12): p. 1103-13.
137. Yokoyama, T., et al., *Angiotensin II and mechanical stretch induce production of tumor necrosis factor in cardiac fibroblasts.* Am J Physiol, 1999. **276**(6 Pt 2): p. H1968-76.

138. Miyoshi, M., et al., *ANG II is involved in the LPS-induced production of proinflammatory cytokines in dehydrated rats.* Am J Physiol Regul Integr Comp Physiol, 2003. **284**(4): p. R1092-7.
139. Ji, Y., et al., *Angiotensin II induces inflammatory response partly via toll-like receptor 4-dependent signaling pathway in vascular smooth muscle cells.* Cell Physiol Biochem, 2009. **23**(4-6): p. 265-76.
140. Kular, L., et al., *The CCN family: a new class of inflammation modulators?* Biochimie, 2011. **93**(3): p. 377-88.
141. Moritani, N.H., et al., *Comparable response of ccn1 with ccn2 genes upon arthritis: An in vitro evaluation with a human chondrocytic cell line stimulated by a set of cytokines.* Cell Commun Signal, 2005. **3**(1): p. 6.
142. Nozawa, K., et al., *Connective tissue growth factor promotes articular damage by increased osteoclastogenesis in patients with rheumatoid arthritis.* Arthritis Res Ther, 2009. **11**(6): p. R174.
143. Abraham, D.J., et al., *Tumor necrosis factor alpha suppresses the induction of connective tissue growth factor by transforming growth factor-beta in normal and scleroderma fibroblasts.* J Biol Chem, 2000. **275**(20): p. 15220-5.
144. Yu, F., C.W. Chou, and C.C. Chen, *TNF-alpha suppressed TGF-beta-induced CTGF expression by switching the binding preference of p300 from Smad4 to p65.* Cell Signal, 2009. **21**(6): p. 867-72.
145. Rittie, L., et al., *Spatial-temporal modulation of CCN proteins during wound healing in human skin in vivo.* J Cell Commun Signal, 2011. **5**(1): p. 69-80.
146. Ago, T. and J. Sadoshima, *GDF15, a cardioprotective TGF-beta superfamily protein.* Circ Res, 2006. **98**(3): p. 294-7.
147. Kang, P.M. and S. Izumo, *Apoptosis and heart failure: A critical review of the literature.* Circ Res, 2000. **86**(11): p. 1107-13.
148. McDonald, T.E., et al., *Endotoxin infusion in rats induces apoptotic and survival pathways in hearts.* Am J Physiol Heart Circ Physiol, 2000. **279**(5): p. H2053-61.
149. Neviere, R., et al., *Caspase inhibition prevents cardiac dysfunction and heart apoptosis in a rat model of sepsis.* Am J Respir Crit Care Med, 2001. **163**(1): p. 218-25.
150. Li, H.L., et al., *Lipopolysaccharide induces apoptosis in adult rat ventricular myocytes via cardiac AT(1) receptors.* Am J Physiol Heart Circ Physiol, 2002. **283**(2): p. H461-7.

151. Frantz, S., et al., *Toll4 (TLR4) expression in cardiac myocytes in normal and failing myocardium.* J Clin Invest, 1999. **104**(3): p. 271-80.
152. Comstock, K.L., et al., *LPS-induced TNF-alpha release from and apoptosis in rat cardiomyocytes: obligatory role for CD14 in mediating the LPS response.* J Mol Cell Cardiol, 1998. **30**(12): p. 2761-75.
153. Sandra, F., et al., *TNF inhibited the apoptosis by activation of Akt serine/threonine kinase in the human head and neck squamous cell carcinoma.* Cell Signal, 2002. **14**(9): p. 771-8.